ORNL
MASTER COPY

OAK RIDGE NATIONAL LABORATORY

operated by

UNION CARBIDE CORPORATION

for the

U.S. ATOMIC ENERGY COMMISSION

ORNL-TM-81

89

CHEMICAL TECHNOLOGY DIVISION

CHEMICAL DEVELOPMENT SECTION B

QUARTERLY PROGRESS REPORT

JULY–SEPTEMBER 1961

NOTICE

This document contains information of a preliminary nature and was prepared primarily for internal use at the Oak Ridge National Laboratory. It is subject to revision or correction and therefore does not represent a final report. The information is not to be abstracted, reprinted or otherwise given public dissemination without the approval of the ORNL patent branch, Legal and Information Control Department.

LEGAL NOTICE

This report was prepared as an account of Government sponsored work. Neither the United States, nor the Commission, nor any person acting on behalf of the Commission:

A. Makes any warranty or representation, expressed or implied, with respect to the accuracy, completeness, or usefulness of the information contained in this report, or that the use of any information, apparatus, method, or process disclosed in this report may not infringe privately owned rights; or

B. Assumes any liabilities with respect to the use of, or for damages resulting from the use of any information, apparatus, method, or process disclosed in this report.

As used in the above, "person acting on behalf of the Commission" includes any employee or contractor of the Commission, or employee of such contractor, to the extent that such employee or contractor of the Commission, or employee of such contractor prepares, disseminates, or provides access to, any information pursuant to his employment or contract with the Commission, or his employment with such contractor.

ORNL-TM-81

CHEMICAL TECHNOLOGY DIVISION

Chemical Development Section B

QUARTERLY PROGRESS REPORT FOR CHEMICAL DEVELOPMENT SECTION B

JULY-SEPTEMBER, 1961

R. E. Blanco

DATE ISSUED

JAN 26 1962

OAK RIDGE NATIONAL LABORATORY
Oak Ridge, Tennessee
Operated by
UNION CARBIDE NUCLEAR COMPANY
for the
U.S. ATOMIC ENERGY COMMISSION

ABSTRACT

Graphite Fuels

Greater than 99% of the uranium and thorium was recovered from unirradiated 1.5-in-dia Pebble Bed reactor fuel spheres by leaching with boiling 90% HNO_3 if the sphere was not coated with SiC or the fuel particles were not coated. High uranium recoveries from spheres coated with pyrolytic carbon were achieved only after rough crushing of the spheres. Both SiC and pyrolytic carbon were inert to 90% HNO_3. The 90% HNO_3 method, while not applicable to the processing of fuels containing coated fuel particles, is being tested as a destructive method for evaluating the integrity of the particles coatings, either before or after irradiation. The graphite matrix is disintegrated exposing the particles to nitric acid. Any uranium or thorium solubilized is a measure of the damage undergone by the particles.

Uranium Carbides

Hydrolysis in water at 80°C of a uranium monocarbide-uranium metal specimen containing 17 mole % U metal yielded 2 moles of free hydrogen per mole of metal in addition to the expected hydrocarbon products. Scouting studies with a specimen containing considerable amounts of U_2C_3 (some UC_2 and either U metal or UC) showed that the gaseous hydrolysis products at 80°C consisted of 58% hydrogen, 2% methane, 26% ethane, and a complex mixture of 24 additional saturated and unsaturated hydrocarbons. The best synthesis of UC_2 by the ORNL Metallurgy Division was a specimen with a combined-C/U atom ratio of 1.73.

Beryllium and Beryllium-Oxide

Dissolution of sintered BeO-5% UO_2 in HF-HBF_4 solutions containing up to 5 M HBF_4 was studied. The initial dissolution rate increased from about 0 to 1.4 mg min^{-1} cm^{-2} as the HF concentration increased from 0 to 15 M regardless of the HBF_4 concentration. GCRE fuel pellets (70% UO_2-30% BeO) were completely dissolved in less than 14 hr in boiling 8 M HNO_3 containing 0.5-0.8 M NaF. The final solution contained about 4 g of uranium per liter.

Dissolution of Zirconium in Titanium Equipment

Continuous dissolution of Zircaloy-2 in a titanium dissolver appears practical on a chemical basis where the steady state dissolver solution is refluxing 3 M HNO_3-0.4 M HBF_4-0.6 M Cr (III)-0.4 M Cr(VI)-0.46 M Zr 1.2 M HF. Dissolution and corrosion rates are 10 mg/cm^2-min and 0.0 mil/mo in short term tests, respectively. A stable product solution containing 0.36 M Zr is obtained after addition of aluminum nitrate to complex fluoride ion. Another reagent investigated for use in continuous dissolution is 16 M HNO_3-2.6 M F-0.025 M HBF_4-1.4 M Zr with titanium corrosion rates of 0.0 mil/mo. However, Zircaloy-2 dissolution rates are only 3 mg/cm^2-min in the latter reagent.

Simultaneous Processing of MTR and Zr-U Alloy Fuels

Solution stability studies indicate that MTR and Zr-U alloy fuel dissolver solutions can be mixed and processed simultaneously in a solvent extraction plant. An equal volume mixture would result in a solution containing 0.7 M Al, 1 M H, 0.65 M Zr, 4 M F, 0.009 M Si, 0.003 M Sn, and about 3 g/l U. Simultaneous processing would result in higher plant capacity and a smaller waste volume.

Modified MTR Recovery Flowsheet

Laboratory experiments indicate that the use of a MTR recovery flowsheet with an acid deficient feed and a divided acid scrub instead of the present acid feed and aluminum nitrate scrub would increase decontamination by a factor >2. However, when the flowsheet was changed so that present equipment could be used without modification, the increased decontamination was no longer observed.

Coextraction of Uranium, Thorium, and Protactinium

Preliminary studies have shown that TBP will extract uranium, thorium, and 40% of the protactinium from synthetic thorium fuel solution with decontamination factors from rare earth elements, ruthenium, and zirconium-niobium of 10^5, 180, and 3.7, respectively.

Adsorption of Protactinium on Glass

The amount of protactinium removed from nitric acid solutions containing 6×10^5 c/m/ml Pa by 15 min batch equilibrations with 10 g 100-200 mesh unfired vycor glass per liter, increased from 82% in 0.1 M HNO_3 to a maximum of 94% in 6 to 8 M HNO_3. Experiments with 6 M HNO_3 showed the adsorption was more than 90% complete in the first 5 min of contact. The presence of 50 g Th/l decreased the adsorption of 0.1 to 8 M HNO_3 to 57 and 86%, respectively, but increased the adsorption in acid deficient solutions from 0 to 45%. About 90% of the protactinium was removed by passing 20 ml of a solution containing 2×10^5 c/m/ml Pa, 220 g Th/l, 15 g U/l, 0.09 M Al, 0.04 M F and 9-10 M HNO_3 through a column containing 1/2 g of 100-200 mesh unfired vycor glass. A column of fired vycor did not remove protactinium from the solution.

Niobium Extraction Studies

The aqueous to organic distribution coefficient of niobium-95 between 0.1 N AD to 4 M HNO_3 and 30% freshly purified TBP in n-dodecane ranged from ~0.004 to ~0.05 with $>$ 90 to 70% of the niobium unextractable. The organic to aqueous coefficient ranged from 0.015 to 0.1 with $<$10% of the activity retained by the organic. When the organic solutions also contained 3% degraded TBP and 7% degraded Amsco, the maximum extraction was obtained at 4 M HNO_3. The aqueous to organic distribution coefficient was 0.4 with $<$10%.

unextractable and the organic to aqueous value was 0.6. The maximum retention by the solvent was about 40% and was attained when the aqueous was 0.1 N HNO_3.

Corrosion Studies

Types 304L and 347 stainless steel corroded at maximum overall rates of 0.50 and 0.19 mil/mo, respectively, in proposed Modified Zirflex solvent extraction media at 50°C. Both showed localized attack after 700 hr exposure. Haynes 25 was attacked uniformly by CCl_4 in N_2, the log of the weight loss varying inversely as 1/T (°K) from 12.4 mg/cm^2·day at 540°C to 1006 at 730°C. Type 347 stainless steel corroded at a maximum rate of 0.02 mil/mo in 2 M acetic acid, 1 M HNO_3, 45 g/l $UO_2(NO_3)_2 \cdot 6H_2O$. Titanium corroded at a maximum rate of 0.03 mil/mo in 20 M HNO_3 containing 50 g of dissolved uranium and 20 g of solid graphite per liter. Haynes 25 corroded at a maximum rate of 0.31 mil/mo in Darex dissolver solution. There was some sign of intergranular attack.

Zirconium, Zircaloy-2 and Hastelloy B corroded at maximum rates of 0.7, 0.9, and 6.7 mils/mo, respectively, in flowing 6 M HCl, 0.0015 M H_2O_2 at 105°C.

Foam Separation

The surface chemistry and foaming properties of dodecylbenzene sulfonate were studied with respect to the use of this surfactant in a foam process for decontaminating ORNL low level waste. Using tap water as a substitute for the waste, the saturated surface concentration of the sulfonate by both static and single stage foam column methods was found to be (3.1-3.4) 10^{-10} moles/cm^2, the critical micelle concentration in the bulk phase 2.2 x 10^{-3} moles/liter, and foam stability down to < 0.08 x 10^{-3} moles/liter, i.e., at <4% of the CMC. At calcium concentrations of 0-4 ppm, sodium hydroxide concentrations of (5 or 10) x 10^{-3} M, and sulfonate concentrations of 62 to 250 mg/liter, strontium distribution coefficients, Γ/x, (foam/bulk solution) ranged from (1-20) x 10^{-3} cm. On the basis of a practical value of Γ/x = 2.5 x 10^{-3} cm and a foam column of ~20 theoretical stages, the calculated decontamination factor is >10^2 for a volume reduction of 10^2, a throughput of ~50 gal ft^{-2} hr^{-1}, and a bubble diameter of 0.5 mm.

Phosphate Glasses

Simulated TBP-25 waste was incorporated into glassy solid products by fluxing at 875-1000°C with phosphite, borate and lead. Densities and volume reduction factors varied from 2.36 to 2.84 and from 7.6 to 8.4, respectively. The addition of lead as fluxing agent was found to have no deleterious effect upon the fixation of ruthenium in the solid by hypophosphite. Silver, mercuric, and palladium ions were found to catalyze the phosphite-nitrate reaction.

Gas-liquid equilibria and solution densities were measured over a series of concentrations of TBP-25, high sulfate Purex and Darex waste solutions.

Low-Level Waste Treatment

An eighth demonstration run in the semi pilot plant facility gave d.f.'s >1000 for Sr, 100 for TRE and >100 for Cs prior to breakthrough at ~1500 bed volumes. Overall volume reduction was slightly less than 3000. Total hardness averaged 20 ppm. The early breakthrough experienced in the seventh run is believed to have been due to carbonate deficiency in the feed which resulted in saturation of the resin with calcium from $Ca(OH)_2$. This will be forestalled in the pilot plant by continuous analysis of hardness in the effluent.

Fission Product Recovery by Ion Exchange

Recovery of strontium and rare earths by ion exchange is being tested at high flow rates in order to find optimum processing conditions to minimize the residence time of the fission product activity on the resin bed. The solution being tested is a treated 1WW-Purex waste containing < 10% and ~30% of the original iron and aluminum, respectively, and < 15% of the original sulfate. In the first experiment at a flow rate of 15 ml/min, or 3 cm/min linear velocity, 97% of the rare earths and 40% of the strontium were sorbed on the resin bed. Citrate elution of rare earths was contaminated with ~15% of the total sorbed Sr^{85} activity while versenate elution of strontium was contaminated with ~25% of the total sorbed Ce^{144}-Pr^{144} activity.

Radiation Damage to Ion Exchange Resin

Amberlite 200 resin, after a dose of 0.97×10^9 r in flowing water, lost 34% of its original capacity, comparable to Dowex 50W X-8 resin which lost 30% of its original capacity after a dose of 0.85×10^9 r. The radiolytic loss of sulfur, G(-S), for Amberlite 200 was calculated to be 1.2. Other analyses indicated that moisture content had increased from its original 53% to 57%, median pore diameter had increased from 250 Å to 315 Å and surface area had increased from 50 to 60 m^2/g dry resin.

Chemical Application of Nuclear Explosions

Oxygen-bearing salts and oxides were found to be good catalysts for tritium exchange in the reaction, $HTO + H_2 \longrightarrow HT + H_2O$ at a temperature of 600°C. Chlorides were found to be ineffective. Fine powders of $CaSO_4$ gave erratic results in kinetic studies of the exchange which was apparently due to compaction of the powder to a slightly porous plug. The mechanism of reduction of $MgSO_4$ and of $CaSO_4$ by H_2 at 750 to 900°C appears to be that the sulfates are first reduced to sulfites which subsequently decompose to the oxide and SO_2. The final reduction products are governed by the thermodynamics of reactions among the metal oxide, H_2, H_2O, and SO_2.

CONTENTS

		Page
1.0	FUEL DISSOLUTION	6
1.1	Graphite Fuels	6
1.2	Uranium Carbides	9
1.3	Beryllium and Beryllium Oxide	13
1.4	Dissolution of Zirconium in Titanium Equipment	15
2.0	SOLVENT EXTRACTION STUDIES	17
2.1	Simultaneous Recovery of MTR and Zr-U Alloy Fuels	17
2.2	Extraction of MTR Fuel Solution Using Acid Scrub and Acid Deficient Feed	18
2.3	Coextraction of Protactinium, Uranium and Thorium	21
2.4	Adsorption of Protactinium on Vycor Glass	22
2.5	Niobium Extraction Studies	22
3.0	CORROSION STUDIES	32
3.1	Modified Zirflex System	32
3.2	Gas Solid Reaction Processing Schemes	32
3.3	Plutonium Solvent Extraction System	33
3.4	Graphite Fuel Decomposition Studies	35
3.5	Darex System	36
3.6	Transuranium Reprocessing System	36
4.0	MECHANISMS OF SEPARATIONS PROCESSES - FOAM SEPARATION	37
4.1	Surface Chemistry of Dodecyl Benzene Sulfonate	37
4.2	Low Level Waste Decontamination	40
5.0	WASTE TREATMENT	42
5.1	Phosphate Glasses	42
5.2	Ruthenium Volatility	43
5.3	Nitrate-Phosphite Reaction	43
5.4	Waste Solution Vapor-Liquid Equilibrium Data	44
5.5	Low Level Waste Treatment	44
6.0	ION EXCHANGE	44
6.1	Fission Product Recovery by Ion Exchange	44
6.2	Radiation Damage to Ion Exchange Resin	45
7.0	CHEMICAL APPLICATIONS OF NUCLEAR EXPLOSIONS	47
7.1	Tritium Exchange	47
7.2	Reduction of Sulfates by Hydrogen	48
8.0	REFERENCES	50

1.0 FUEL DISSOLUTION
(L. M. Ferris)

1.1 Graphite Fuels (L. M. Ferris and A. H. Kibbey)

The 90% HNO_3 process (1) was tested on full-size unirradiated Pebble Bed reactor fuel spheres fabricated during Sanderson and Porter's fuel element development program (2). The 1.5-in.-dia spheres disintegrated readily in boiling 90% HNO_3 providing that they were not coated with SiC or pyrolytic carbon. Uranium and thorium recoveries in two, 4-hr leaches were greater than 99% if the fuel particles were not coated or the sphere not coated with SiC. To achieve high recoveries from pyrolytic carbon-coated spheres, rough crushing prior to acid leaching was required.

Three experiments with uncoated spheres confirmed prior work (3) in that uranium and thorium were nearly quantitatively recovered from the graphite matrix when the fuel particles are not coated. After 2, 4-hr leaches with boiling 90% HNO_3 at least 99% of the uranium and thorium was recovered from spheres FA-19 (~8% U) and FA-15 (~1% U and 9% Th) which were simple dispersions of 150-micron UC_2 and ThC_2-UC_2 particles, respectively, in a graphite matrix (Table 1).

Table 1. Disintegration of Pebble Bed Reactor Fuel with 90% HNO_3

Sphere Code		Recoveries, %					
		First Leach		Second Leach		Residue	
		U	Th	U	Th	U	Th
FA-19	UC_2 particles	99.44	-	0.5	-	0.06	-
FA-15	UC_2-ThC_2 particles	93.6	94.5	5.8	5.4	0.6	0.15
FA-24	Pyrolytic carbon-coated UC_2 particles	1.6	-	4.3	-	94.1	-

On the other hand, only 5.9% of the uranium was recovered from specimen FA-24 (~8% U) which contained pyrolytic carbon-coated UC_2 fuel particles. Specimen FA-24 was, like the other specimens, completely disintegrated by a 4-hr 90% HNO_3 treatment.

As expected, silicon carbide-coated spheres were not penetrated by boiling 90% HNO_3. Moreover, even after rough crushing only about 86% of the uranium was recovered from specimen FA-8 by the standard, two-leach treatment with boiling acid. This specimen contained 7.85% uranium as uncoated 100- to 200-micron UC_2 particles dispersed in a ball which had a SiC coating 30 mils thick. The overall silicon content was 17.5%. In the first 4-hr leach of

the crushed specimen, 83.1% of the uranium was recovered. Another 3.4% of the uranium was recovered in the second leach leaving 13.5% unrecovered in the residue. It remains to be determined whether the unrecovered uranium was chemically combined with the SiC or whether this type of fuel requires a longer leaching period.

Spheres coated with pyrolytic carbon also were inert to boiling 90% HNO_3 over long periods of time. Tests with specimen FA-21, a sphere with a 50 mil pyrolytic carbon coating containing about 8% uranium as uncoated UC_2 particles dispersed in a graphite matrix, showed that the 50-mil coating was not penetrated after 20 hr exposure to boiling acid and 16 hr exposure at room temperature. After 40 hr of contact, cracks appeared in the coating and disintegration of the matrix began. After penetration of the coating, leaching with boiling 90% HNO_3 for 4.5 hr recovered 87.8% of the uranium. In a second 6.3-hr leach, an additional 11.2% of the uranium was recovered leaving 0.94% in the residue. This test indicates that the 90% HNO_3 method will probably result in adequate uranium recoveries from crushed pyrolytic carbon-coated elements if they do not contain coated fuel particles.

Since fuel particles coated with either pyrolytic carbon or sintered Al_2O_3 are not markedly affected by boiling 90% HNO_3, this method is being evaluated as a technique for determining the integrity of coated fuel particles dispersed in graphite matrices before and after irradiation. The matrix is disintegrated exposing the coated fuel particles to nitric acid. Any uranium or thorium leached is therefore a measure of the damage that the particles have undergone.

Several leaching tests were conducted with pyrolytic carbon-coated UC_2 particles. Small samples (0.5 to 1 g) were digested twice for 6 hr with boiling nitric acid, either 8 or 21.2 M, before analysis of the solutions and the residue. Two batches of particles, 3M-D and NCC-J, Type A containing about 69 and 44% uranium, respectively, were used in the tests. Digestion for 6 hr with 8 M HNO_3 resulted in the leaching of only about 10^{-3}% of the uranium from each type of particle (Table 2). A 6-hr treatment with boiling 90% HNO_3, however, resulted in considerably more solubilization of the uranium, particularly with the NCC batch. Specifically, about 0.3% was leached from 3M-D samples while over 11% was leached from the NCC samples (Table 2). The amount of uranium leached by 90% HNO_3 was increased by about a factor of 3 during the second leach. This behavior suggests that the 90% HNO_3 treatment not only reflects the extent to which the coatings are damaged but also results in some oxidation of the coatings. The extent of damage would be indicated mainly by the first leach data since the rate of oxidation of the coatings has been shown to be very slow. It is also possible that the apparent disagreement among the first leach data from the 8 and 21.2 M HNO_3 experiments arises from the difference in rate of dissolution of UC_2 at different acid concentrations. The final appraisal of the 90% HNO_3 treatment for evaluating the relative integrity of the coatings must await corroborating data from an independent method such as fission gas release measurement.

Table 2. Leaching of Pyrolytic Carbon-coated UC_2 Particles with Boiling Nitric Acid

Each leach, 6 hr

Batch	U Content of Particles, %	HNO_3 Conc, M	Uranium Solubilized, % First Leach	Uranium Solubilized, % Second Leach
3M-D	-	8	0.003	-
NCC-J	-	8	0.001	-
3M-D	69.24	21.2	0.34	2.5
3M-D	68.58	21.2	0.33	1.0
NCC-J	44.00	21.2	11.8	35.8
NCC-J	43.86	21.2	11.5	36.4

It is significant, however, that both 3M[s] and NCC particles although dispersed in a graphite matrix, behave in a manner predictable from the tests with unsupported particles. Tests were conducted on 4, unirradiated hollow cylindrical graphite pellets containing pyrolytic carbon-coated UC_2 particles similar to those used in the tests described above. Pellets 91 and 110 from batch ORR- CP-3M and pellets 16 and 75 from batch NC-UC-6 were disintegrated and leached for 6 hr with boiling 90% HNO_3. The powdered residues were washed thoroughly with water after the acid treatment. These tests show again that the 3M particles were quite resistant to 90% HNO_3 (10^{-4} to 10^{-2}% of the uranium leached) while those from NC (about 25% of the uranium leached) apparently had undergone severe damage or the coatings were readily oxidized (Table 3).

Table 3. 90% HNO_3 Leaching of Graphite Pellets Containing Pyrolytic Carbon-coated UC_2 Particles

Each pellet leached 6 hr with boiling acid

Batch	Pellet No.	Uranium in Pellet, %	Uranium Leached, %
ORR-CP-3M	91	12.6	1.2×10^{-2}
ORR-CP-3M	110	9.56	9.4×10^{-4}
NC-UC-6	16	8.91	26.8
NC-UC-6	75	9.63	24.7

1.2 Uranium Carbides (M.J. Bradley)

Commercially manufactured uranium monocarbide fuels will almost certainly contain either uranium metal or excess carbon as higher carbide impurites (4). In addition the HTGR and Pebble Bed proposals call for uranium dicarbide in graphite as the fuel. The hydrolysis behavior of uranium metal dispersed in the monocarbide, uranium sesquicarbide, and uranium dicarbide thus is equally as important as the chemistry of the monocarbide.

All carbide specimens were prepared by arc melting high purity uranium metal (less than 400 ppm total impurities) and spectroscopic grade graphite.* Specimen U_2C_3-1A was heat-treated at about 1600°C for 60 hr to transform the high temperature stable compounds, UC and UC_2, to the low temperature form of U_2C_3. Specimen 6B by elemental analysis contained about 17 mole % uranium metal dispersed throughout the monocarbide matrix, while specimen U_2C_3-1A was close to the theoretical composition for uranium sesquicarbide (Table 4). Photomicrographs of U_2C_3-1A showed the presence of large amounts of two additional phases in the sesquicarbide matrix. It was the opinion of the metallography group that one phase etched like UC_2,** and from the chemical analysis it is obvious that UC_2 cannot be present without uranium metal and/or monocarbide also being present. Little unreacted carbon was detected in either sample.

Table 4. Chemical Analysis of Uranium Carbides

Specimen No.	Elemental Analysis, mmoles per g			Combined-C/U Atom Ratio
	U	Total C	Free C	
6B	4.03	3.33	0.04	0.83
U_2C_3-1A	3.91	5.77	0.03	1.47

Uranium Monocarbide-Uranium Metal Dispersion

Hydrolysis, at 80°C, of a specimen containing 17 m/o uranium metal dispersed in a uranium monocarbide matrix yielded an insoluble hydrous uranium oxide and 106 ml (STP) of gas per gram of sample consisting of about 36 v/o hydrogen, 60 v/o methane, and small quantities of the higher hydrocarbons (Table 5). More than 24 hr were required for complete hydrolysis of a 5-g specimen compared to only 3 hr for the hydrolysis of the monocarbide at the same temperature (Fig. 1). The hydrogen concentration increased from 20 v/o in the first gas sample to about 50 v/o in the third (last) with a corresponding decrease in the methane concentration from 80 to 50 v/o. These results indicate that uranium metal reacts more slowly than uranium monocarbide with water.

---

*D. W. Bourgette, ORNL Metallurgy Division.
** R. J. Gray, ORNL Metallurgy Division.

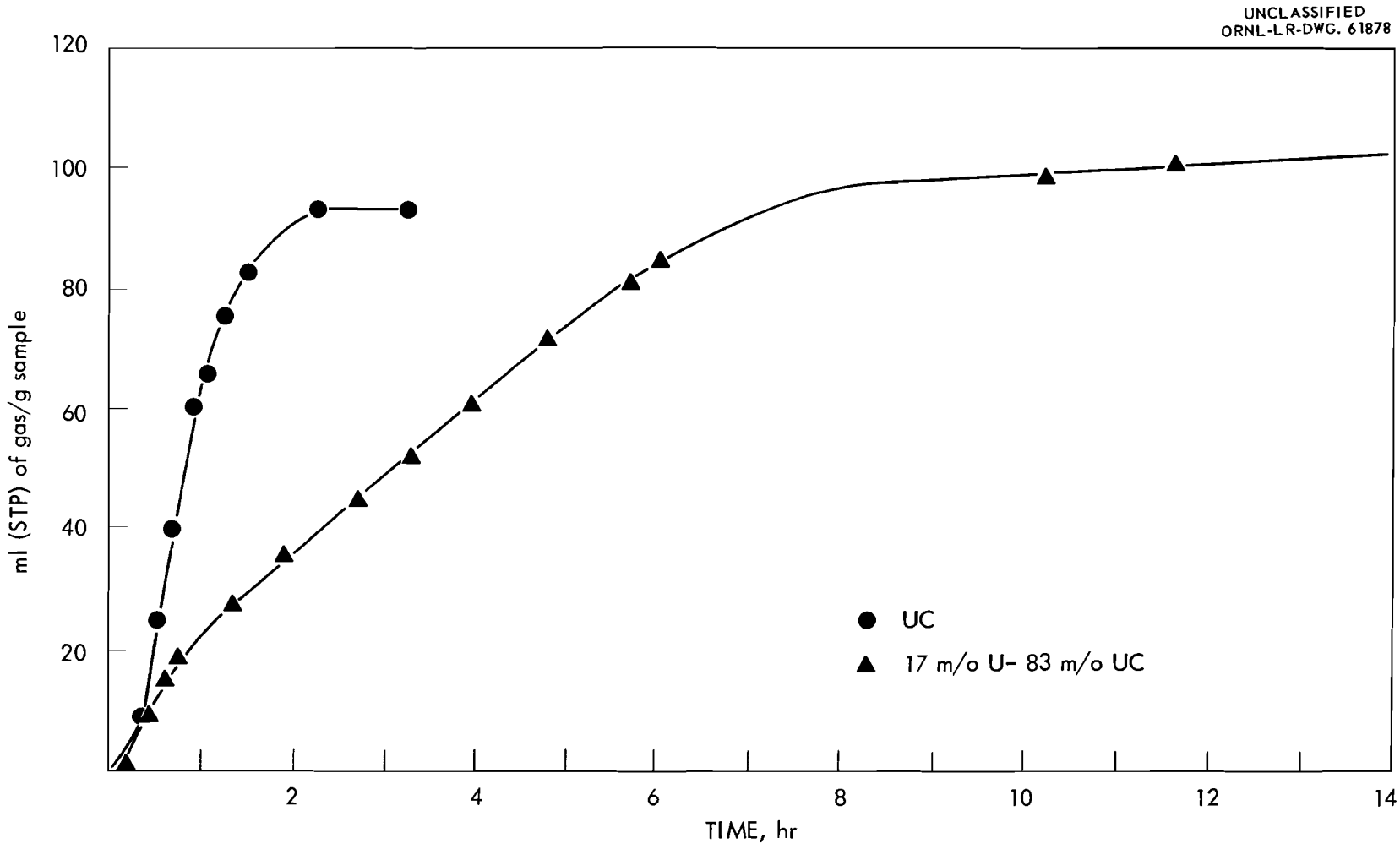

Fig. 1. Effect of uranium metal impurity on rate of hydrolysis of UC at 80°C.

The hydrous uranium oxide was not readily soluble in 6 N HCl at 80°C; 10% of the uranium was insoluble after 2 hr and about 3% insoluble after 16 hr. In contrast, the solid hydrolysis product from uranium monocarbide dissolved completely in 6 N HCl at 80°C within an hour. The residue from hydrolysis of the specimen containing 17 m/o uranium metal was soluble in boiling 12 M H_3PO_4. Analysis of the resulting solutions showed that at least 95% of the uranium was in the tetravalent state.

A complete material balance for carbon and uranium was obtained. For each gram of specimen 6B hydrolyzed (4.03 mmoles of U and 3.33 mmoles of C) there was found 3.31 mmoles of monatomic carbon (2.83 in CH_4 and 0.48 in C_2-to C_6-hydrocarbons) and 16.06 mmoles of monatomic hydrogen (3.43 as H_2, 11.34 in CH_4 and 1.29 in C_2-C_6 hydrocarbons).

Thus in addition to the expected uranium monocarbide products (5), there was produced 2 mmoles of free hydrogen for each mmole of uranium metal. As in the case of near stoichiometric uranium monocarbide, the hydrocarbons above methane may be the result of free radical polymerization of intermediate UC hydrolysis products, or they may represent U_2C_3 impurities in the specimen.

Table 5. Reaction of Uranium Monocarbide-Uranium Metal Dispersion with Water at 80°C

Composition of specimen 6B given in Table 4

Run No.	Total Volume of Gas, ml/g	Total Carbon, mmoles/g	Total Hydrogen, mmoles/g	Volatile Products: Composition of Gas Evolved,[a] v/o						
				H_2	CH_4	C_2H_6	C_3H_8	C_4H_{10}	iso-C_5H_{12}	n-C_5H_{12}
1	104.4	3.26	15.81	35.4	61.2	2.04	0.74	0.35	0.02	0.09
2	106.2	3.29	16.06	40.1	55.2	1.86	1.62	0.73	0.05	0.22
3	106.8	3.39	16.27	33.4	63.4	1.96	0.70	0.22	0.01	0.08
Avg.	105.8	3.31	16.06	36.3	59.9	1.95	1.02	0.43	0.03	0.13

[a]In addition to the values shown, 0.073 v/o of branched hexanes, 0.04 v/o of n-hexane and 0.16 v/o of unidentified compounds were evolved.

Uranium Sesquicarbide (Sample U_2C_3-1A)

Hydrolysis, at 80°C, of specimen U_2C_3-1A yielded an insoluble, hydrous, uranium(IV) compound, a trace of wax, and 57 ml (STP) of gas per gram sample consisting of 58% hydrogen, 2% methane, 26% ethane, and a complex mixture of some 24 additional saturated and unsaturated hydrocarbons of which 11 could be identified positively (Table 6). Nine of the unknowns occur between

n-hexane and n-heptane and may be the saturated, branched heptanes for which standards are not available. Most of these unknown peaks were also present in the products from UC, but they totaled only an estimated 0.02% instead of 2%. The rate of gas evolution was much slower than from UC; over 6 hr were required for complete hydrolysis compared with about 3 hr for UC under similar conditions. Only about half the carbon appeared in the gas phase. No gas was evolved during the dissolution of the uranium residue in 6 M HCl or 12 M H_3PO_4, and the trace of insoluble wax was too small to be weighed. Therefore the missing carbon is probably present in the acidic uranium-bearing solutions. The phosphoric acid solutions did have an unusual odor.

Conclusions cannot be drawn without at least knowing both the purity of the carbide and the complete composition of the gaseous products. The most striking result was the decrease in the methane concentration from 85% with stoichiometric UC to 2% with U_2C_3-1A and the evolution of only half of the carbon as gas.

Table 6. Reaction of U_2C_3-1A with Water at 80°C

Composition given in Table 4

Run No.	189	191	192	Avg.
Total volume of gas (STP), ml/g	61.5	54.7	55.7	57.3
Total carbon, mmoles/g[a]	2.85	2.69	2.65	2.75
Total hydrogen, mmoles/g[a]	10.81	10.01	10.12	10.44
Composition of Gas Produced, Vol %[b]				
H_2	57.4	57.2	58.1	57.6
CH_4	1.84	1.88	1.80	1.84
C_2H_6	27.1	25.9	25.6	26.2
C_3H_8	1.40	1.41	1.51	1.44
n-C_4H_{10}[c]	6.52	7.57	7.26	7.12
cis-butane-2		1.09	1.04	1.06
trans-butene-2	2.08	0.69	0.86	0.78
?		0.59	0.50	0.54
iso-C_5H_{12}	0.058	0.062	0.045	0.055
n-C_5H_{12}	0.65	0.64	0.49	0.59
?	0.12	0.19	0.18	0.16
2,2-dimethylbutane	0.10	0.07	0.08	0.08
?	0.06	0.06	0.05	0.06
2,3-dimethylbutane + 2-methylpentane	0.30	0.33	0.34	0.32
3-methylpentane	0.21	0.22	0.22	0.22
n-C_6H_{14}	0.91	0.93	0.84	0.89
?	0.84	0.83	0.90	0.86
n-C_7H_{16}	0.14	0.17	0.09	0.13
?	0.30	0.33	0.17	0.27

[a]In identified products.
[b]Gases listed in order of elution.
[c]May also include propylene.

This work has been suspended until the sesquicarbide specimen has been further heat treated in hopes of obtaining a more nearly single phase material.

Uranium Dicarbide

The best synthesis of UC_2 by the ORNL Metallurgy Division was a specimen with a combined-C/U atom ratio of 1.73 (Table 7). The nominal composition of this specimen was $UC_{1.93}$, however, after arc melting 12 times, much of the carbon was still present as free graphite. Increasing the amount of total carbon in the specimens actually decreased the amount of combined carbon; the $UC_{2.00}$ specimen had a combined C/U ratio of 1.68, while the $UC_{2.20}$ specimen had a combined C/U ratio of only 1.55. Additional arc melting offers little advantage, since $UC_{2.00}$ after 4 meltings had a ratio of 1.63 compared with 1.68 after 12 meltings. Another specimen of nominal composition $UC_{1.73}$ contained about as much combined carbon (combined ratio = 1.70) as the specimens with much more total carbon. It would appear that the specimens are not being quenched fast enough to retain all of the UC_2 (the stable phase at high temperatures), and that appreciable decomposition to lower carbides and graphite is occurring upon cooling.

Table 7. Uranium Dicarbide Synthesis

Batch	Synthetic Composition C/U Atom Ratio	No. of Remelts	Elemental Analysis, mmoles/g			Combined C/U Atom Ratio
			U	Total C	Free C	
5A	1.73	4	3.87	6.69	1.20	1.42
5B	1.73	8	3.87	6.69	0.13	1.70
UC_2-1A	2.00	4	3.82	7.59	1.35	1.63
UC_2-4A	1.93	12	3.83	7.39	0.77	1.73
UC_2-5A	2.00	12	3.82	7.54	1.11	1.68
UC_2-6A	2.20	12	3.79	8.14	2.27	1.55

1.3 Beryllium and Beryllium-Oxide (K. S. Warren)

High-Beryllia-Content Fuels Dissolution of sintered BeO-5% UO_2 in boiling mixed fluoride solutions is being studied. Initial rates of dissolution in boiling HF-NH_4F solutions were reported previously (5). The effect of using HBF_4 in the place of NH_4F was investigated in a similar series of experiments. The presence of fluoborate ion, in concentrations up to 5 M, did not have a significant effect on the rate in aqueous HF solutions. The initial dissolution rate increased from about 0 to 1.4 mg $min^{-1}cm^{-2}$ as the HF concentration increased from 0 to 15 M regardless of the HBF_4 concentration (Fig. 2). In boiling HBF_4 solutions containing no HF, the initial rate increased only to 0.2 mg $min^{-1}cm^{-2}$ as the HBF_4 concentration increased to 5 M.

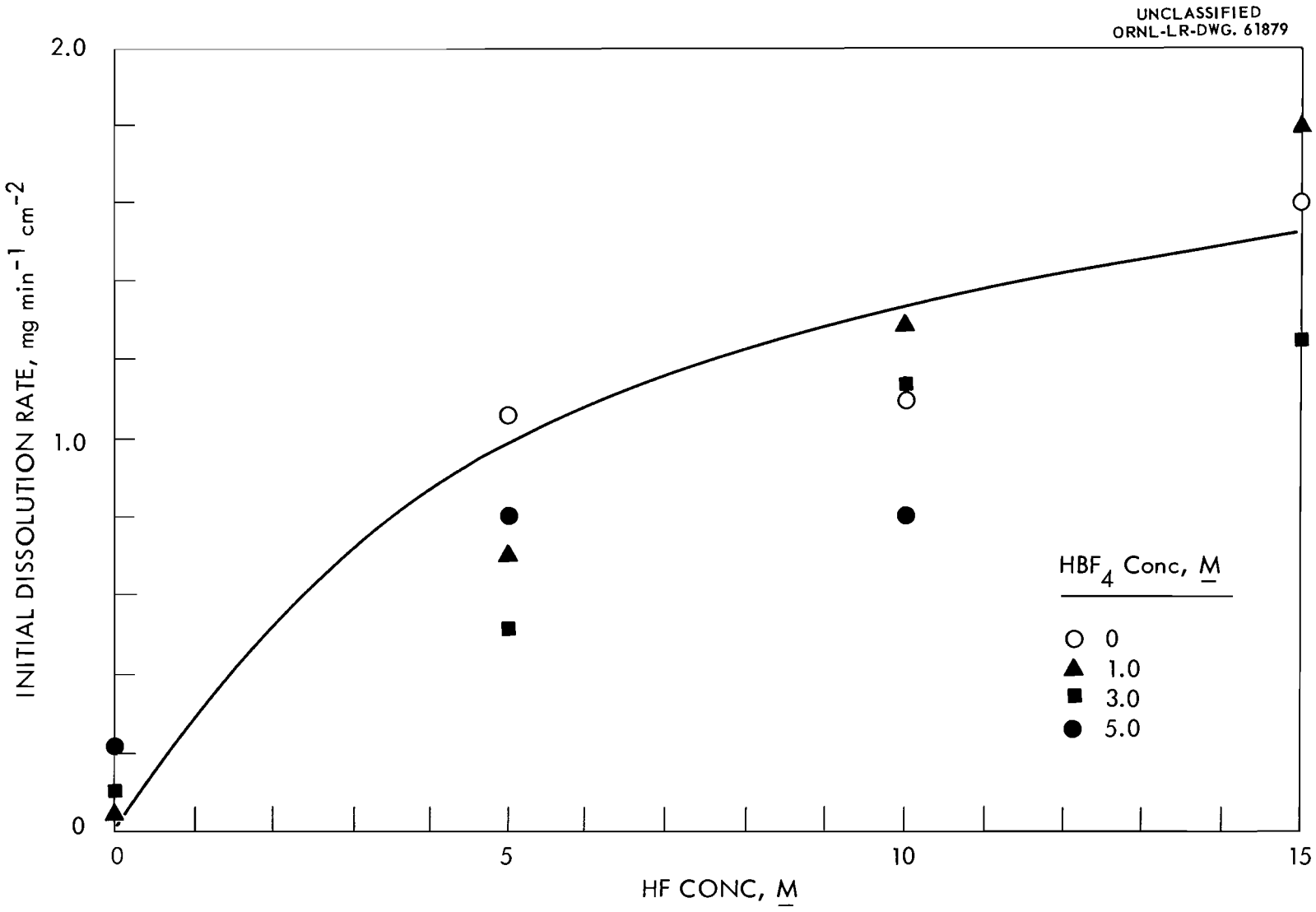

Fig. 2. Initial dissolution rates of sintered BeO-5% UO_2 in boiling HF-HBF_4 solutions. (Curve drawn through points for pure HF solutions only.)

Low-Beryllia-Content Fuels Work has continued on the effect of fluoride ion on the dissolution of GCRE fuel pellets (70% UO_2-30% BeOO in boiling nitric acid solutions. It was shown previously (5) that the presence of sodium fluoride, in concentrations up to 0.2 M, did not decrease the time required for complete dissolution of pellets in boiling 8 M HNO_3. However, recent work has shown that the pellets dissolved completely in 8 M HNO_3 containing 0.5 to 0.8 M NaF in 14 hr or less, which was about half the time required in boiling 8 M HNO_3 alone. The terminal uranium concentration in the solutions produced was about 4 g/liter.

Studies of the dissolution of GCRE fuel pellets in HNO_3-H_2SO_4 solutions were also continued. Prior work (5) showed that the rate at which UO_2 was leached in 6-8 M HNO_3 was not affected by H_2SO_4 in concentrations up to 2 M. On the other hand, the rate of dissolution of the BeO matrix increased with increasing H_2SO_4 concentration. In boiling 7.8 M HNO_3-7.6 M H_2SO_4, however, uranium was leached from the pellet more slowly than with 8 M HNO_3 alone (Fig. 3). About 50% of the UO_2 was dissolved in 8 hr as compared with approximately 1/2 hr in 8 M HNO_3. Dissolution of the BeO matrix was also slower when the solution contained 7.6 M H_2SO_4; 50% dissolved in 12 hr whereas in 8 M HNO_3 alone only about 8 hr was required to effect the same extent of dissolution. The results of these tests show that the maximum rate of dissolution of both the UO_2 and BeO portions of the fuel is achieved in 8 M HNO_3-2 M H_2SO_4.

A GCRE fuel pellet which had been ground to pass through a 100 mesh screen required 18 hr for complete dissolution in boiling 8 M HNO_3. This dissolution time is about half that required for whole-pellet dissolution. The final solution contained about 4 g of uranium per liter in each case.

1.4 Dissolution of Zirconium in Titanium Equipment

The utility of a Darex (6) titanium dissolver would be greatly extended if the titanium vessel could be used in dissolution of reactor fuels containing zirconium as well as stainless steel. Since fluoride must be used in any practical aqueous dissolution of zirconium fuels, inhibition of the attack of fluoride on titanium using strong nitric acid, chromate, and fluoboric acid, singly or in combinations, was studied. All of these methods of inhibition have been briefly investigated previously (7,8). The most promising chromium reagent found was dilute nitric-hydrofluoric acid containing both hexavalent and fluoboric acid to inhibit titanium corrosion. Strong nitric-hydrofluoric acid with a small amount of fluoboric acid produces a more desirable solvent extraction feed solution but requires closer control of the reagent composition and does not dissolve Zircaloy rapidly.

In a solution of 3 M HNO_3-0.4 M HBF_4-1.2 M HF-0.46 M $(NH_4)_2Cr_2O_7$ films form on the surface of both the titanium and zirconium but only the titanium is protected significantly by its film. Results vary widely with the experimental conditions. Titanium corroded at a rate of 1 in./mo in fresh reagent, but the corrosion rates decreased very rapidly with zirconium loading.

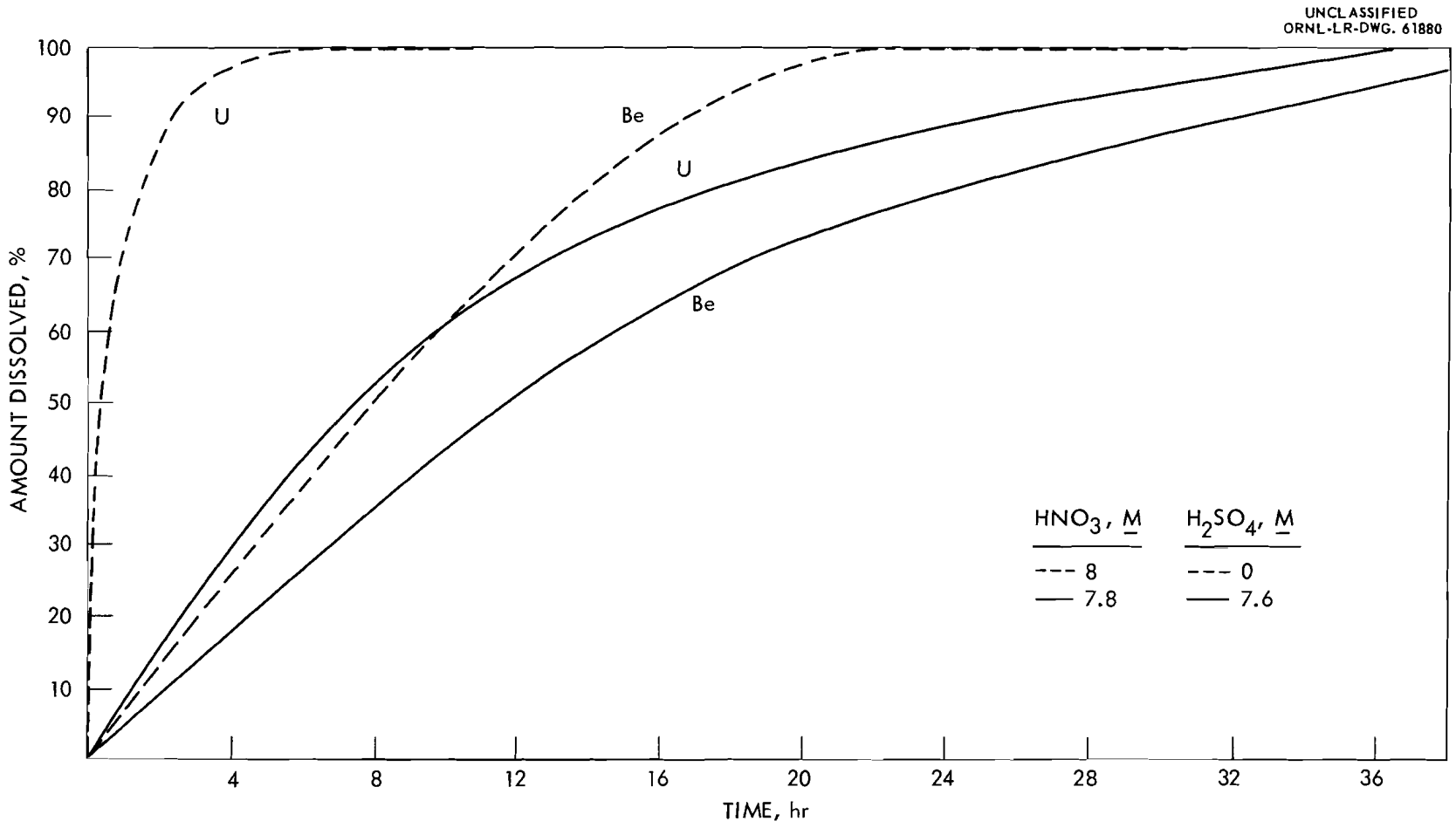

Fig. 3. Dissolution of GCRE fuel pellet in boiling acid mixtures.

Most promising results were obtained with dissolving zirconium coupled to titanium where, at a F/Zr solution ratio of 26, the zirconium dissolution rate exceeded 30 mg/cm^2-min and the titanium corrosion rate was 0.0 mil/mo. Without coupling, the titanium corrosion rate dropped to 0.0 mil/mo when the F/Zr solution ratio decreased to 9, where the zirconium dissolution rate still exceeded 20 mg/cm^2-min. No off-gas was observed during dissolution, the net reaction apparently being oxidation of Zircaloy-2 metal and reduction of Cr(VI) to Cr(III). The product solutions appear to be stable at a loading of 0.47 M Zr (F/Zr = 6) but precipitation occurs at higher loadings. Inadvertant stopping of the feed reagent does not appear to be a serious problem, although it appears that all of the Cr(VI) in the residual dissolver solution could be reduced during dissolution of the excess zirconium metal present, to produce a Zr concentration of about 0.7 M at a F/Zr ratio of 4. Actually, this point would never be reached since the zirconium becomes coated at a F/Zr ratio of 5.5, ~0.5 M Zr, and dissolution ceases. Hence an excess of Cr(VI) will always be present. Three major problems require detailed studies:

1) Preparation of a noncorrosive, stable solvent extraction feed solution;
2) Examination of the system under continuous dissolving conditions. Behavior of the surface films cannot be predicted with confidence from batch data.
3) A method of continuously measuring and controlling product composition. Since the fluoride concentration is fixed by the feed solution, maintence of a zirconium concentration high enough to hold the F/Zr ratio within the required limits is mandatory. Density measurement appears adequate for corrosion control, but is not sensitive enough to ensure close control of zirconium concentration to minimize the excess of fluoride used and total product volume.

A detailed report is being processed (9).

2.0 SOLVENT EXTRACTION STUDIES
(R. H. Rainey)

2.1 Simultaneous Recovery of MTR and Zr-U Alloy Fuels (R. H. Rainey and J. W. Ullmann)

Laboratory experiments indicate that MTR and Zr-U alloy could be processed simultaneously in the Idaho Chemical Processing Plant, resulting in a decrease in operating time and waste volume. These fuels are presently being processed separately.

The uranium-zirconium alloy fuel is dissolved in hydrofluoric acid. The fluoride is then complexed with aluminum nitrate prior to the solvent extraction of uranium. The MTR fuel is an aluminum clad uranium-aluminum alloy. ICPP has proposed that the aqueous waste from the two processes be combined for storage following uranium recovery. As an alternative, it may be economical

to mix the dissolver solution prior to extraction and thus increase plant capacity and eliminate the addition of aluminum as a complexing agent. Equal volume mixtures of the two dissolver solutions result in a feed for the solvent extraction plant which is essentially identical to the present Zr-U alloy solvent extraction feed solution except for presence of silica from the MTR and a higher concentration of uranium. The higher uranium concentration can easily be accomodated by minor changes in the solvent extraction flowsheet. Laboratory experiments were made to determine the range of stability of mixtures of the two solutions.

A synthetic MTR fuel solution was prepared by dissolving a piece of MTR end plate containing brazing material in nitric acid catalyzed with mercuric nitrate. The solution was then adjusted to MTR dissolver solutions conditions by adding uranyl nitrate and diluting with water. The adjusted solution analyzed 1.4 M $Al(NO_3)_3$, 0.25 N acid deficient, 1.55 g/l U, and 0.02 g/l silicon. This solution should have been about 1 M HNO_3 to duplicate ICPP conditions.

The synthetic Zr-U alloy solution was prepared by dissolving a piece of the alloy in hydrofluoric acid, then diluting with water. An analysis of the solution showed 1.13 M Zr, 0.006 M Sn, 1.43 g/l U, 1.08 M HNO_3, and 7.0 M F.

The stability was determined by warming the two solutions to 80°C then preparing mixtures having MTR/Zr-U alloy volume ratios of 0.75, 1.0, 1.5, 2.0, 2.5, 3.0, and 3.5 (Table 8). After standing 3 hr a slight haze of precipitate appeared in each mixture. After 24 hr the 2.5 and 3.0 ratio contained a large amount of precipitate, all other samples contained only a slightly hazy material. No additional change appeared after storage for 6 weeks.

2.2 Extraction of MTR Fuel Solution Using Acid Scrub and Acid Deficient Feed (R. H. Rainey)

In laboratory experiments the use of an acid scrub and an acid deficient feed instead of aluminum nitrate scrub and acid feed as used in the present MTR-ICPP flowsheet, results in an increase of at least a factor of 2 in the decontamination from ruthenium and zirconium-niobium. The use of an acid scrub in a flowsheet which could be used without modification of the present Idaho Chemical Processing Plant did not result in improved decontamination. Laboratory experiments are continuing to determine the decontamination when using a flowsheet which would require only minor piping modifications.

A series of countercurrent batch extraction experiments have been made to determine the decontamination of synthetic MTR fuel when various scrub and feed acidities were used in otherwise identical conditions (Table 9). The MTR flowsheet (11) used as a control was as follows:

Feed: 1.5 g/l U, 1.0 M HNO_3, 1.6 M $Al(NO_3)_3$, 1 volume
Scrub: 0.7 M $Al(NO_3)_3$, 0.2 volume
Extractant: 3.5% TBP in Amsco, 0.75 volume
Stages: 3 extraction, 4 scrub

The use of a neutral feed did not result in a measurable difference in the decontamination, but when the feed was acid deficient and treated with bisulfite,* decontamination from ruthenium and zirconium-niobium were increased about a factor of two. Similarly when an acid feed was used and the scrub was 4 M HNO_3 instead of 0.7 M $Al(NO_3)_3$ the decontamination from ruthenium was increased by about a factor of two but decontamination from zirconium-niobium was not changed. When the pregnant organic was scrubbed first with 4 M HNO_3 then with water, ruthenium in the product was decreased to the limit of analytical detection (increase in decontamination by greater than a factor of 2) and the decontamination from zirconium-niobium was increased by about a factor of two. When an acid deficient feed and a divided scrub were used, the ruthenium and zirconium-niobium in the product were both reduced to below the limit of analytical determination (greater than a factor of 2).

The process engineers at Idaho (11) evaluated the use of an acid scrub and proposed the following conditions which could be used without modification of their present equipment.

Flowsheet No. 1
Described above as present conditions

Flowsheet No. 2
Feed: same as No. 1.
Scrub: 4 M HNO_3, 0.065 volume
Extractant: 3.5% TBP in Amsco, 0.43 volume
Stages: 5 extraction, 2 scrub

Flowsheet No. 3.
Feed: same as No. 1
Scrub No. 1: 8 M HNO_3 at scrub stage No. 2, 0.11 volume
Scrub No. 2: H_2O at scrub stage No. 3, 0.11 volume
Extractant: 5% TBP in Amsco, 0.75 volume
Stages: 4 extraction, 3 scrub

These conditions differ from those previously evaluated in that they have fewer scrub and more extraction stages and that 5% rather than 3.5% TBP was used in the flowsheet having a water scrub in order to decrease uranium reflex.

Duplicate series of experiments using different feed solutions for each series, demonstrated that the experiments using acid scrub did not result in as high decontamination as present conditions (Table 10).

*Bisulfite treatment used to increase decontamination from ruthenium (12).

Table 8. Stability of Mixtures of Synthetic MTR and Zr-U Alloy Dissolver Solutions

	MTR Solution	Zr-U alloy Solution	Present Zr-U Alloy Feed Soln (10)	Volume Ratio of Mixtures MTR/Zr-U Alloy .75	1.0	1.5	2.0	2.5	3.0	3.5
Aluminum	1.4	-	0.78	0.60	0.70	0.84	0.93	1.00	1.05	1.08
Acid N	0.25 AD	1.08	1.0	0.51	0.36	0.28	0.19	0.13	0.08	0.05
Zirconium M	-	1.13	0.5	0.65	0.57	0.45	0.38	0.32	0.28	0.25
Fluoride M	-	7.0	3.3	4.00	3.50	2.80	2.33	2.00	1.75	1.55
Tin M	-	0.006	0.006	0.0034	0.0030	0.0024	0.0020	0.0017	0.0013	0.0013
Silicon g/l	0.02	-	-	0.009	0.010	0.012	0.013	0.014	0.015	0.016
Uranium g/l	1.55	1.43	1.2	1.48	1.49	1.50	1.51	1.51	1.52	1.52
	Stable	Stable	Stable	Stable	Stable	Stable	Stable	Unstable	Unstable	Stable

Table 9. Comparison of the Effect of Various Scrub and Feed Conditions on Decontamination when Using the MTR Flowsheet

Flowsheet	Decontamination Factor				Acid in Organic Product	Uranium Loss
	Gr γ	Ru	Zr-Nb	TRE		
Present	40,000	13,000	40,000	$5x10^6$	0.02 N	.007%
Present	80,000	9,000	100,000	$2x10^6$	0.02 N	.007%
4 M H Scrub	70,000	25,000	100,000	$1x10^6$	0.10 N	.07%
Divided Scrub	100,000	40,000	250,000	-	0.02 N	.23%
Neutral Feed	30,000	7,000	40,000	$2x10^6$	0.02 N	.006%
A.D. Feed	200,000	60,000	200,000	$2x10^6$	0.02 N	.007%
A.D. Feed and Divided Scrub	200,000	40,000	250,000	$1x10^6$	0.03 N	0.10%

Table 10. Use of Acid Scrub in Unmodified MTR Fuel Processing Equipment

Flowsheet	Decontamination Factor				Acid in Organic Product	Uranium Loss
	Gr γ	Ru	Zr-Nb	TRE		
Present	15,000	30,000	8,000	$4x10^6$	0.02 N	.054%
4 N H Scrub	1,000	25,000	250	$4x10^6$	0.05 N	.016%
Divided Scrub	7,000	10,000	1,500	$3x10^6$	0.02 N	.007%
Present	70,000	30,000	30,000	$5x10^6$	-	
4 N H Scrub	25,000	40,000	9,000	$2x10^6$	0.06 N	
Divided Scrub	15,000	15,000	5,000	$6x10^6$	0.02 N	

Duplicate series of experiments using different feed solution for each series.

2.3 Coextraction of Protactinium, Uranium and Thorium (R. H. Rainey)

Processes are being investigated for the simultaneous recovery of protactinium, uranium, and thorium from used thorium reactor fuel. The objective of this work is to achieve quantitive recovery of uranium, thorium and protactinium with modest decontamination since refabrication must be remote in any event. The best results from preliminary experiments show extraction of uranium, thorium, and 40% of the protactinium with a decontamination factor from ruthenium of 180, and from rare earths of 10^5 (Table 11). Decontamination from zirconium-niobium was 3.7. The protactinium which did not extract was in a much less extractable form and may be the result of the method of preparation

of the protactinium tracer solution.

The thorium, uranium, and protactinium was extracted with 30% TBP in Amsco from a feed containing varying concentrations of aluminum nitrate and nitric acid. The best separation of protactinium from ruthenium and rare earth elements was obtained when the feed was ~1 M $Al(NO_3)_3$, ~3 M HNO_3, and the scrub was ~1 M $AlNO_3$, ~4 M HNO_3. The low separation from zirconium-niobium in this process does not constitute a serious disadvantage because these materials have a low neutron cross-section.

Part of the protactinium tracer was readily extractable and part was largely unextractable. In the experiment in which the feed was 1 M $Al(NO_3)$-3 M HNO_3 and the scrub was 1 M $Al(NO_3)_3$-1 M HNO_3 the distribution coefficient of the protactinium in the scrub section was 4 whereas at the first extraction stage it was 1.1 and at the last stage 0.04.

2.4 Adsorption of Protactinium on Vycor Glass (J. G. Moore)

Batch experiments indicate that unfired vycor glass may be used to remove protactinium from nitric acid solutions. Solutions of 0.1 N acid deficient to 10 M HNO_3 and containing ~6 x 10^5 c/m/ml Pa were contacted 15 min with 10 g of 100-200 mesh unfired vycor glass/liter. Although none of the protactinium was removed from the acid deficient solution, 82 to 94% was removed from the acidic solutions (Fig. 4). A similar series in which 50 g Th/l was present in the solutions showed that the presence of thorium decreased the adsorption of protactinium from solutions containing 0.1 to 8 M HNO_3 to about 57 and 86%, respectively, and increased the adsorption in the acid deficient solution from 0 to 45% (Fig. 4).

Time study experiments showed that in the region of maximum adsorption (around 6 M HNO_3) 93% of the protactinium is removed in the first 5 min of contact. Only 4% additional protactinium is removed by contacting the solution with the unfired vycor for 3 hr (Fig. 5). A longer contact time is required with more dilute acids to achieve equilibrium. In tests using 1 M HNO_3, 72% was removed in 5 min and 89% in 3 hr (Fig. 5).

In the one packed column run made with unfired vycor, about 90% of the protactinium was removed from a solution containing approximately 2 x 10^5 c/m/ml Pa, 220 g/l Th, 15 g/l U, 0.09 M Al, 0.04 M F, and 9-10 M HNO_3. A small amount of solids in the feed plugged the column after 20 ml of the solution had passed through 1/2 of 100-200 mesh unfired vycor. A column using fired vycor did not remove the protactinium from the solution. In batch shake-outs using the same solution, about 59%, 61%, and 67%, of the protactinium was removed by stirring with 10, 20 and 40 g/l of unfired vycor, respectively, for 15 min.

2.5 Niobium Extraction Studies (J. G. Moore)

Studies to determine the distribution of niobium-95 between 0.1 N acid deficient to 4 M HNO_3 and tributyl phosphate solutions have been continued

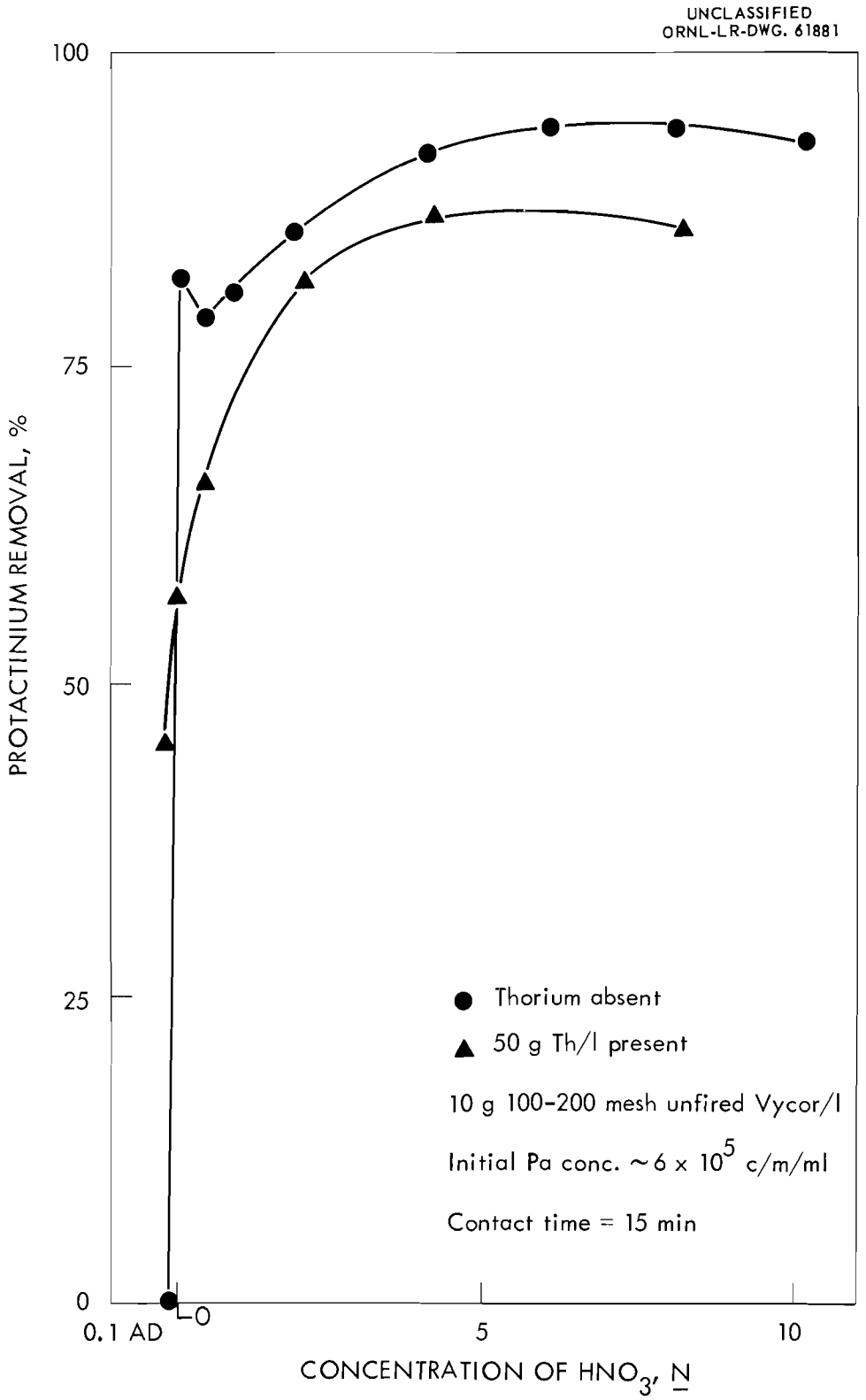

Fig. 4. Protactinium adsorption from nitric acid by unfired Vycor glass.

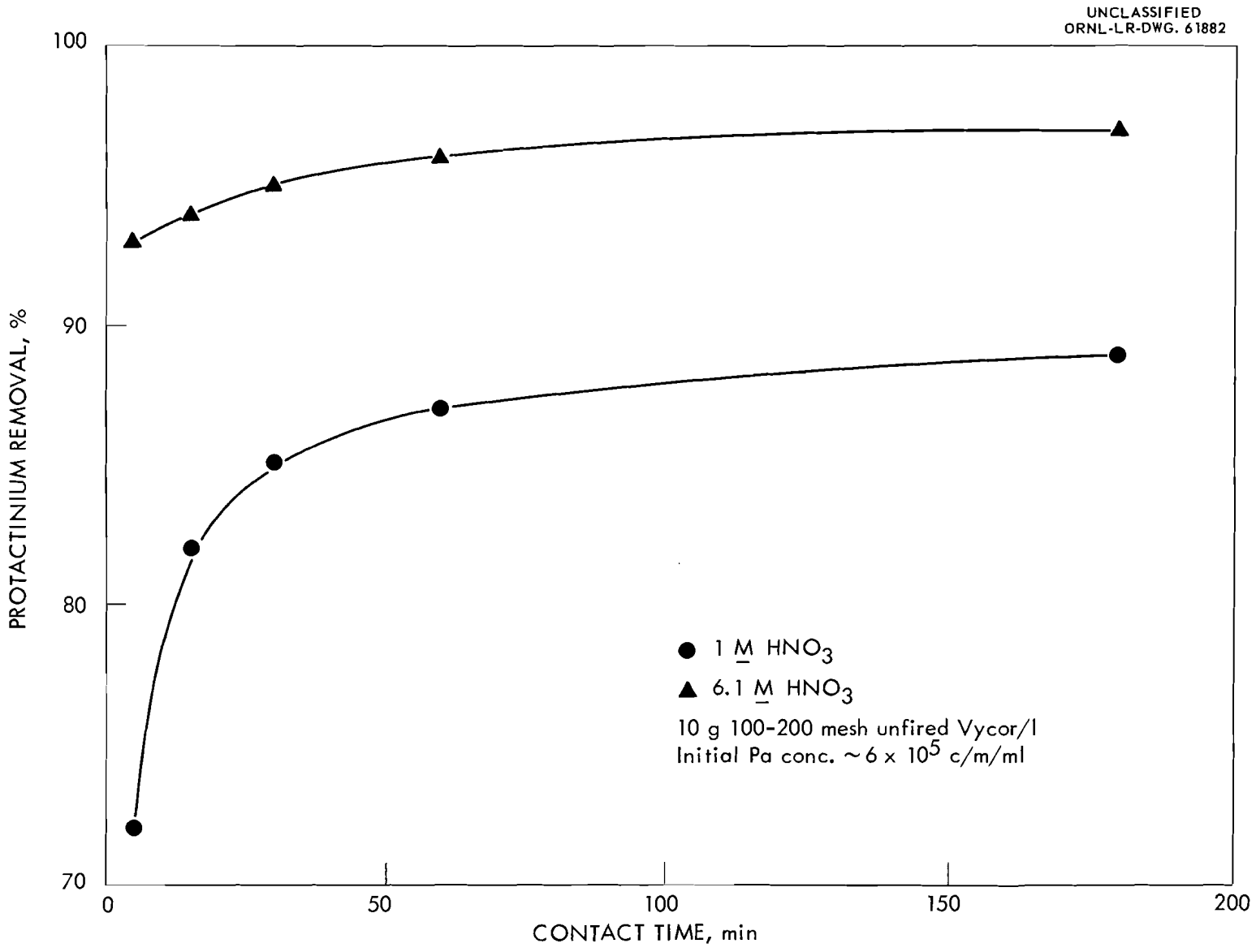

Fig. 5. Protactinium adsorption by unfired Vycor glass as a function of contact time.

Table 11. Simultaneous Extraction of Thorium, Uranium and Protactinium

Flowsheet Conditions:

Feed: 40 g/l Th, 3 g/l U, acid and aluminum as indicated, Pa and FP tracer, 1 volume
Scrub: Acid and aluminum as indicated, 0.4 volume
Extractant: 30% TBP in Amsco, 2 volumes
Stages: 5 extraction, 4 scrub

Exp. No.	Feed		Scrub		Decontamination Factor				Pa % Extracted	Thorium Distribution Coeff.	
	H^+	Al	H	Al	Gr γ	Ru	Zr-Nb	TRE		Feed Plate	4th Scrub
1*	2.87	1.46	2.96	0.81	92	1,400	2.5	38,000	7.1%	6.7	5.7
2*	3.13	1.0	3.93	0.94	6.8	180	3.7	1.3×10^5	41%	-	-
3	2.92	1.05	2.90	0.67	5.5	220	3.0	7,100	7.7%	3.5	4.6
4	2.92	1.05	0.95	1.03	4.9	35	2.3	4,700	8.7%	4.4	12
5	1.54	1.09	0.95	1.03	3.3	4.6	4.5	2,500	52%	4.7	12

*Did not contain fluoride in feed.

using the technique previously described (13). The aqueous to organic distribution coefficient between freshly purified 30% TBP in n-dodecane and nitric acid increased from ~0.004 with 0.07 N acid deficient to ~0.05 with 4.3 M HNO_3. The percent of niobium in an unextractable form decreased from 90% to ~70% as the acid increased (Fig. 6). The organic to aqueous distribution coefficient showed a minimum value of 0.015 at 1 M HNO_3 and increased to ~0.1 at 4 M HNO_3. The amount of niobium retained by the organic ranged from 3 to 8% (Fig. 7). Organic to aqueous data obtained with aqueous solutions containing <0.5 N HNO_3 were so scattered that distribution coefficients could not be calculated.

The distribution coefficient of niobium-95 between nitric acid and an organic phase consisting of 63% n-dodecane, 27% freshly purified TBP, 3% degraded TBP and 7% degraded Amsco increases as the nitric acid concentration increases. The aqueous to organic coefficient ranged from 0.03 in an acid deficient solution to 0.4 in 4 M HNO_3 (Fig. 8). These values were calculated as before (13) using only the straight line portion of the graph obtained by plotting the aqueous vs the organic activity. The curvature of the plots increased as the aqueous acid concentration decreased and at 0.1 M HNO_3 it was impossible to calculate a distribution coefficient by this method. In addition the extrapolated abscissa intercept of the straight line portion indicated negative values (i.e. <0% unextractable niobium) for all tests using less than 4 M HNO_3. The data for 4 M HNO_3 showed that 2 to 6% of the niobium is in an unextractable form.

The organic to aqueous distribution coefficient ranged from 0.03 to 0.6 (Fig. 9). The data showing the activity retained by the organic was scattered but indicated a maximum retention of ~40% in the 0.1 M HNO_3 test (Fig. 10). No explanation has been found for the disagreement of the 4 M HNO_3 results with the previously reported organic to aqueous value of 1.8 and 6.7% retained and aqueous to organic value of 0.8 and 20% unextractable (13). As seen in Figs. 8 and 9, several sets of data were collected for some of the acid conditions to determine the effect of feed pretreatments and different niobium stock solutions. Although there is scatter in the data, especially in the lower acidities, the scatter at 4 M HNO_3 is not sufficient to account for the discrepancy. Because of this discrepancy an attempt was made to reproduce the previously reported values obtained with 1 M HNO_3 and an organic solution containing 27% freshly purified TBP, 3% degraded TBP, and 70% n-dodecane. Experimental results using a different niobium stock solution and a feed pretreatment of 100°C for 1 hr, gave an aqueous to organic value of 0.25 with <0% unextractable compared to the previous value of ~0.35 and 0% unextractable. The organic to aqueous value is 0.33 with 13% retained compared to the previous value of ~0.4 with 0% retained.

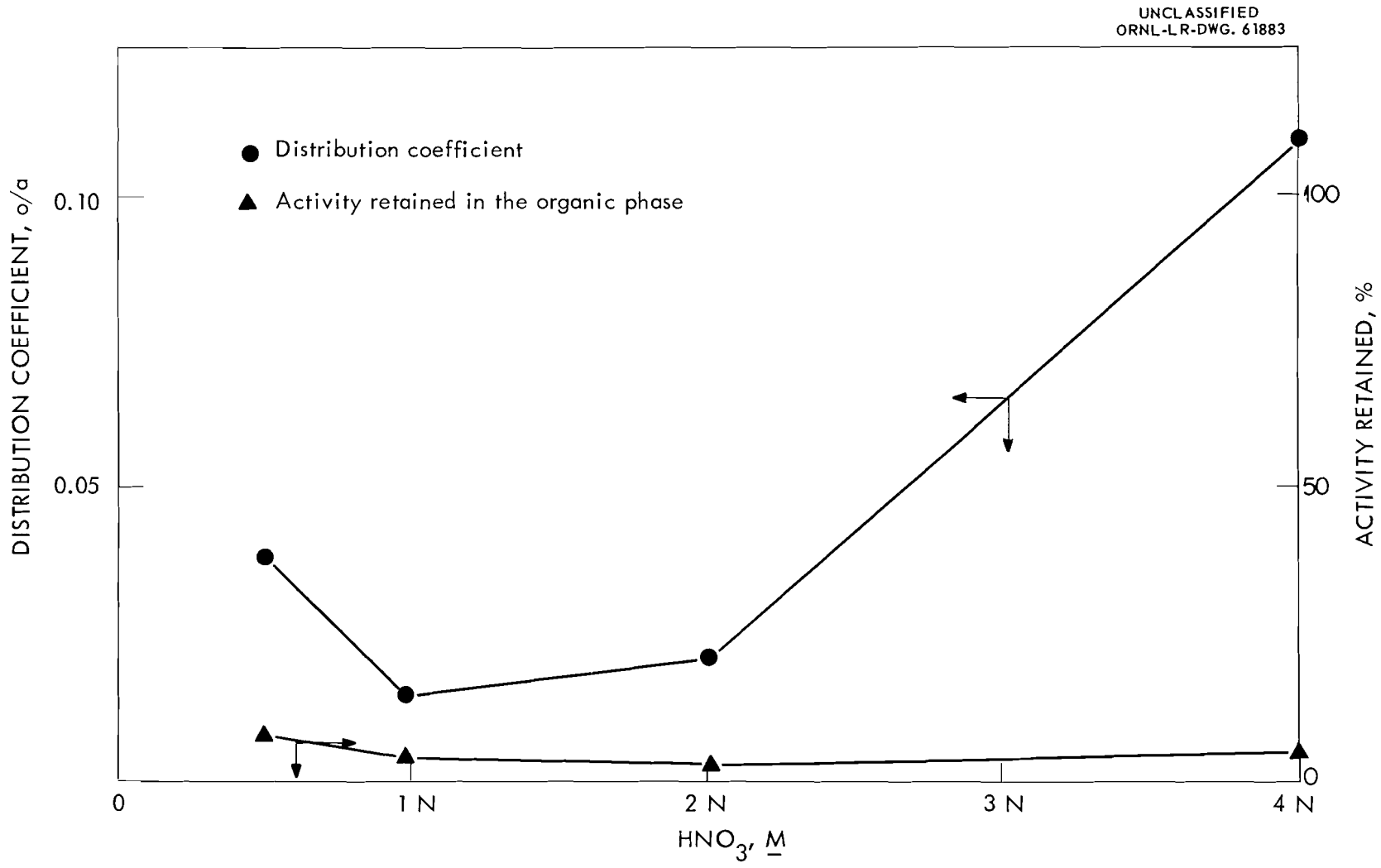

Fig. 6. Organic to aqueous distribution of niobium between nitric acid and 30% freshly purified TBP in n-dodecane.

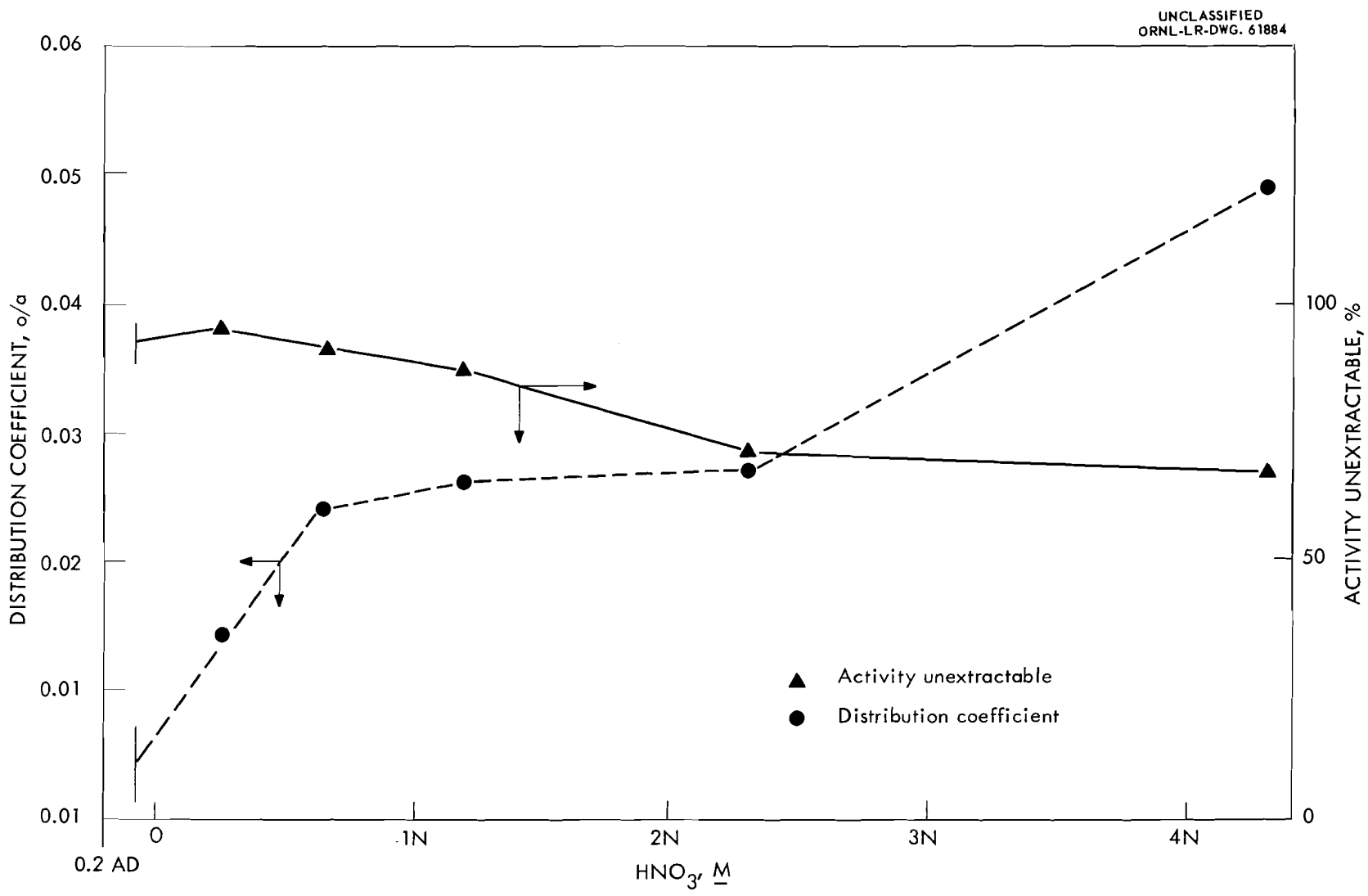

Fig. 7. Aqueous to organic distribution of niobium-95 between nitric acid and 30% freshly purified TBP in n-dodecane.

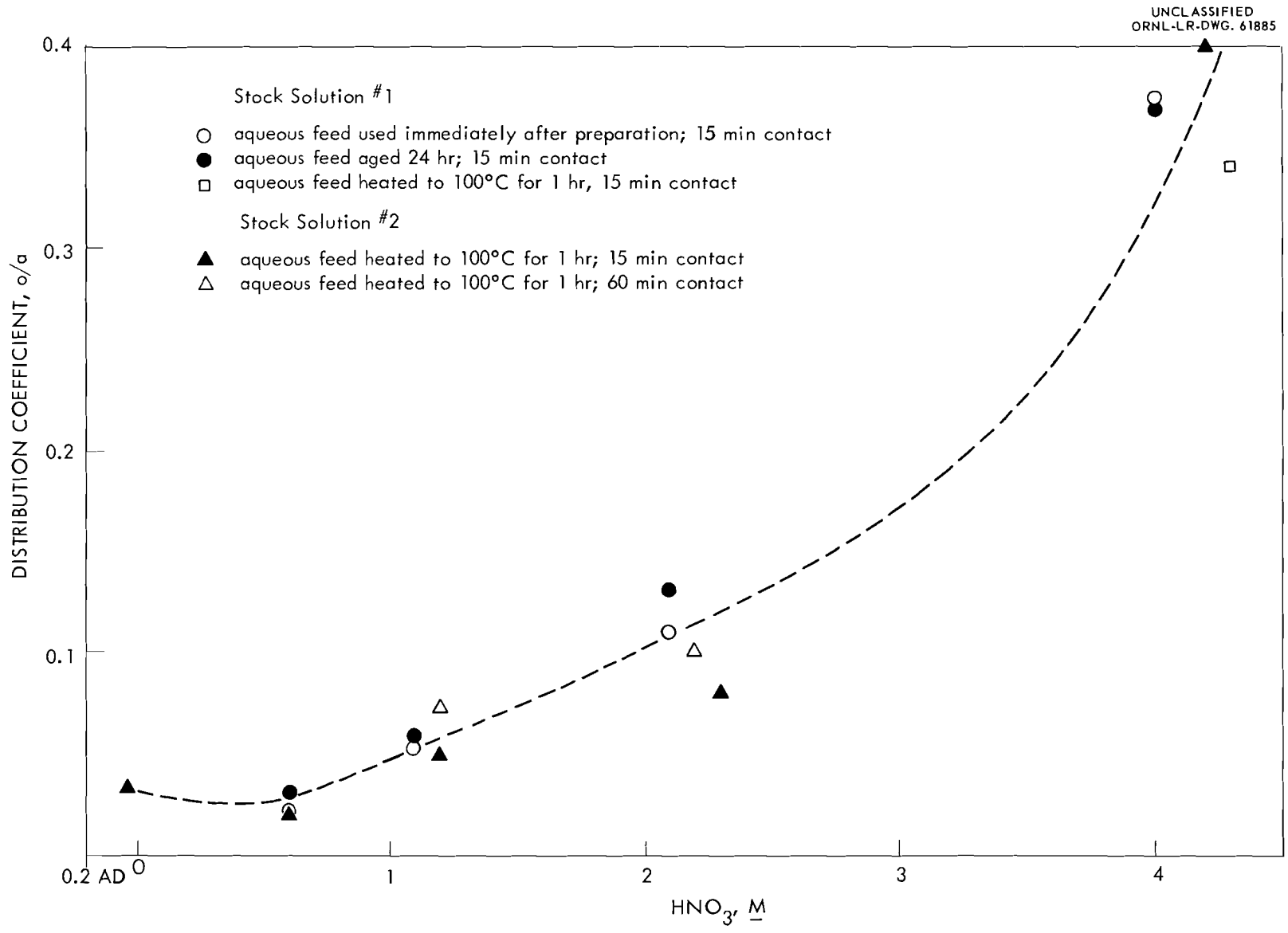

Fig. 8. Aqueous to organic distribution of niobium-95 between nitric acid and an organic solution consisting of 63% n-dodecane, 27% freshly purified TBP, 3% degraded TBP and 7% degraded amsco. TBP and amsco degraded together.

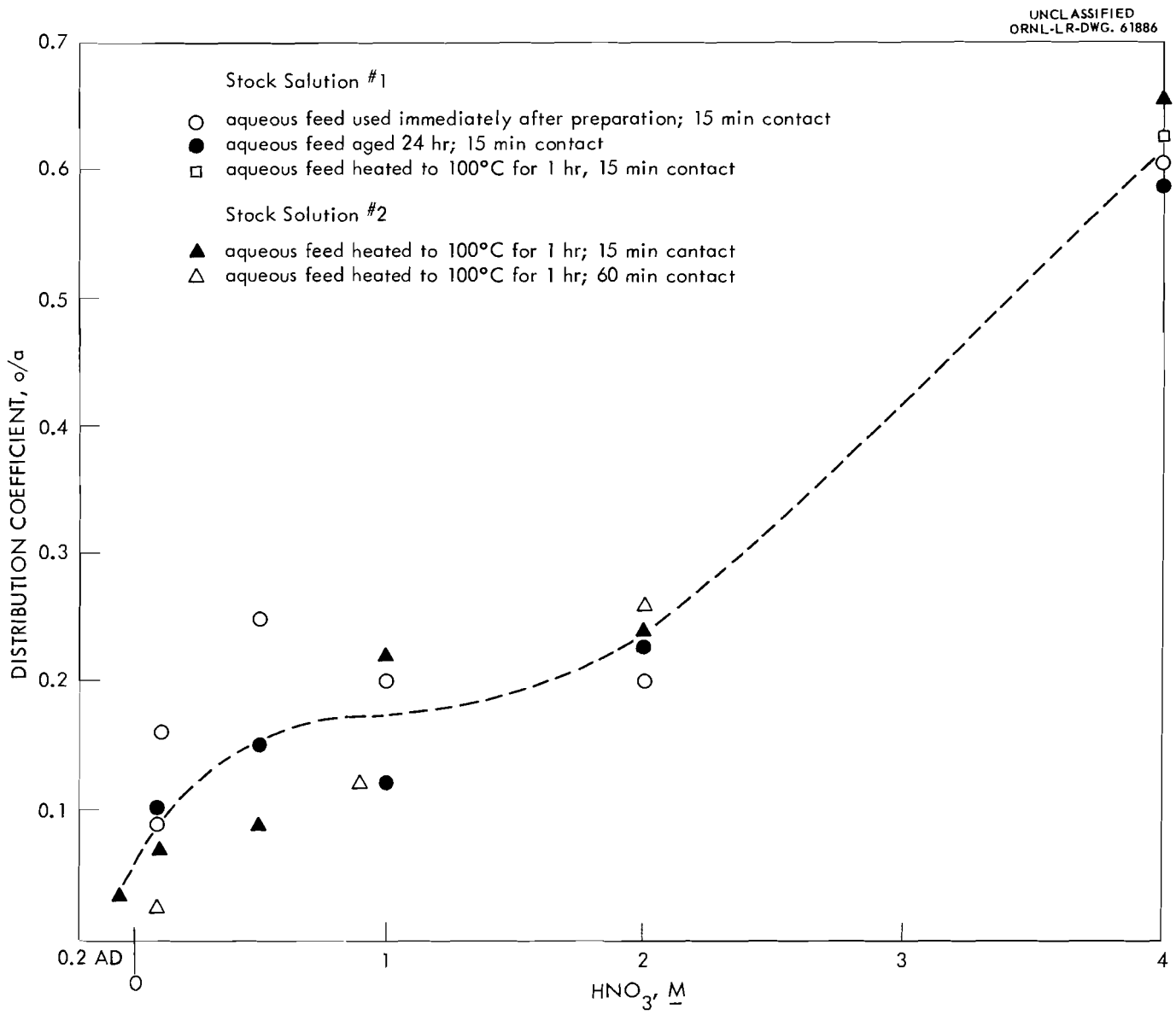

Fig. 9. Organic to aqueous distribution of niobium-95 between nitric acid and an organic solution consisting of 63% n-dodecane, 27% freshly purified TBP, 3% degraded TBP and 7% degraded amsco.

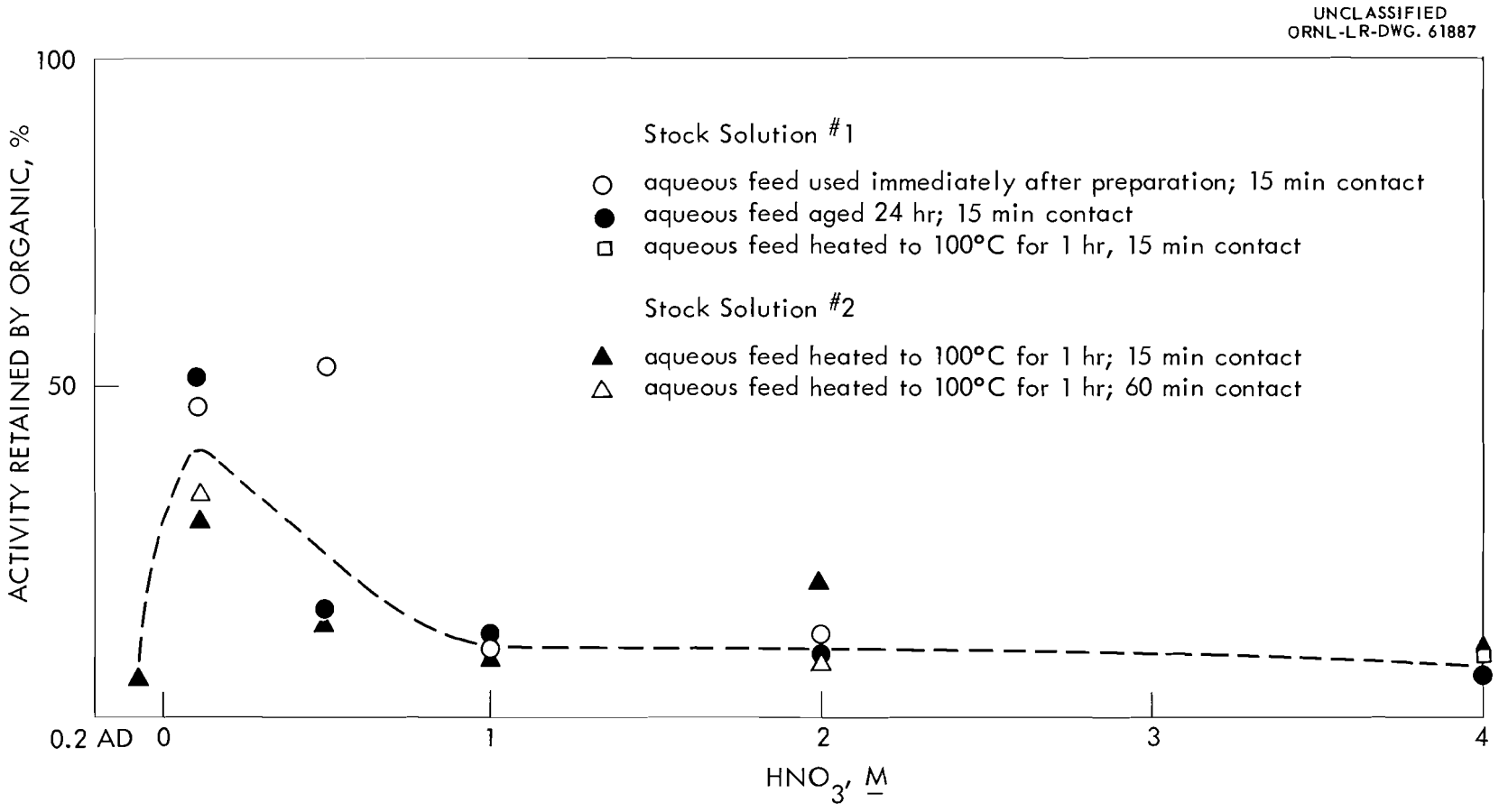

Fig. 10. Niobium-95 retention by an organic solution consisting of 63% n-dodecane, 27% freshly purified TBP, 3% degraded TBP and 7% degraded amsco.

3.0 CORROSION STUDIES

(Work performed by members of the Reactor Chemistry Division, ORNL)

W. E. Clark

Studies have continued on the behavior of stainless steels in proposed Modified Zirflex solvent extraction environments, in gas-solid processing schemes, and in chloride systems proposed for the processing of transuranium elements. In addition, work has been done in proposed systems for the solvent extraction of plutonium, the decomposition of graphite fuels, and on the performance of welded high cobalt alloys in Darex dissolver solution.

3.1 Modified Zirflex System

Continued exposure (700 hr total) of Types 304L and 347 stainless steels in proposed Modified Zirflex solvent extraction solutions (0.75-1.5 M HNO_3, 0.6 M Al^{+3}, 0.36-0.49 M Zr^{+4}) at 50°C resulted in overall maximum rates of 0.49 and 0.19 mil/mo for Type 304L and Type 347, respectively, (Table 12). The specimens of 304L experienced grain boundary attack and some localized etching while the 347 specimens were attack preferentially in the heat-affected zone near the welds and exhibited a general surface-pickling attack.

Table 12. Corrosion of Types 304L and 347 Stainless Steels in Modified Zirflex Solvent Extraction Feed Solutions at 50°C

Solution Composition M					Test Period	Corrosion Rate (mpm)		
HNO_3	Al	Zr	F	Alloy	(hr)	V	I	S
0.75	0.6	0.49	3.33	304L SS	504	0.09	0.31	0.50
					700	0.09	0.24	0.38
0.75	0.6	0.49	3.33	347 SS	504	0.06	0.10	0.13
					700	0.07	0.09	0.10
1.5	0.6	0.36	2.44	304L SS	504	0.11	0.14	0.61
					700	0.11	0.12	0.49
1.5	0.6	0.36	2.44	347 SS	504	0.12	0.13	0.19
					700	0.12	0.13	0.19

3.2 Gas Solid Reaction Processing Schemes

Data previously reported on the corrosion of various alloys in N_2-CCl_4 at elevated temperatures (13) was somewhat anomalous in that it indicated an entirely illogical effect of specimen position on the corrosion rate. Careful measurement of specimen temperatures during testing of Haynes 25 indicates that the specimen temperatures differed at times by as much as

±32°C from the recorded temperature of the furnace (Table 13). The customary kinetic plot of log rate vs 1/T for the corrosion reaction was found to approximate a straight line (Fig. 11), indicating the strong accelerating effect of temperature on corrosion rate and the necessity of cooling the walls of the reactor if this environment is to be applied. Though Haynes 25 showed unacceptably high rates at the higher temperatures the corrosion attack appeared to be uniform.

Table 13. Haynes 25 Temperatures Determined During Passage of Nitrogen-Carbon Tetrachloride Mixture Through Hydrochlorinator Reaction Vessel

Time After Mixture Addition Started (hr)	Temperature (°C) Specimen Position (inches from exit) Upstream 10 1/2	Middle[a] 8 3/4	Downstream 7
A. Temperature of Reaction Vessel ~700°C			
1.0	718	721	666
2.0	718	718	678
16.5	721	732	699
21.5	694	718	678
24.0	704	732	694
Corrosion Rate (mpm)	767.5	1006	267
B. Temperature of Reaction Vessel ~550°C			
1.0	558	560	540
2.0	563	566	543
18.0	558	560	550
24.0	567	561	542
Corrosion Rate (mpm)	15.2	20.6	12.4

[a]Thermocouple used to control furnace temperature.

3.3 Plutonium Solvent Extraction System

A tube of 347 stainless steel containing steam at 25 psig (heat transfer ≅5000 Btu/hr·ft^2) was exposed for 96 hr in a solution consisting of 1 M HNO_3, 2 M acetic acid, 45 g/l $UO_2(NO_3)_2 \cdot 6H_2O$. The tube suffered only a mild acid etch. Coupon specimens exposed in the solution, vapor, and interface positions showed maximum rates of 0.02 mil/mo (Table 14). It appears therefore, that Type 347 stainless steel can be safely used for construction of this equipment.

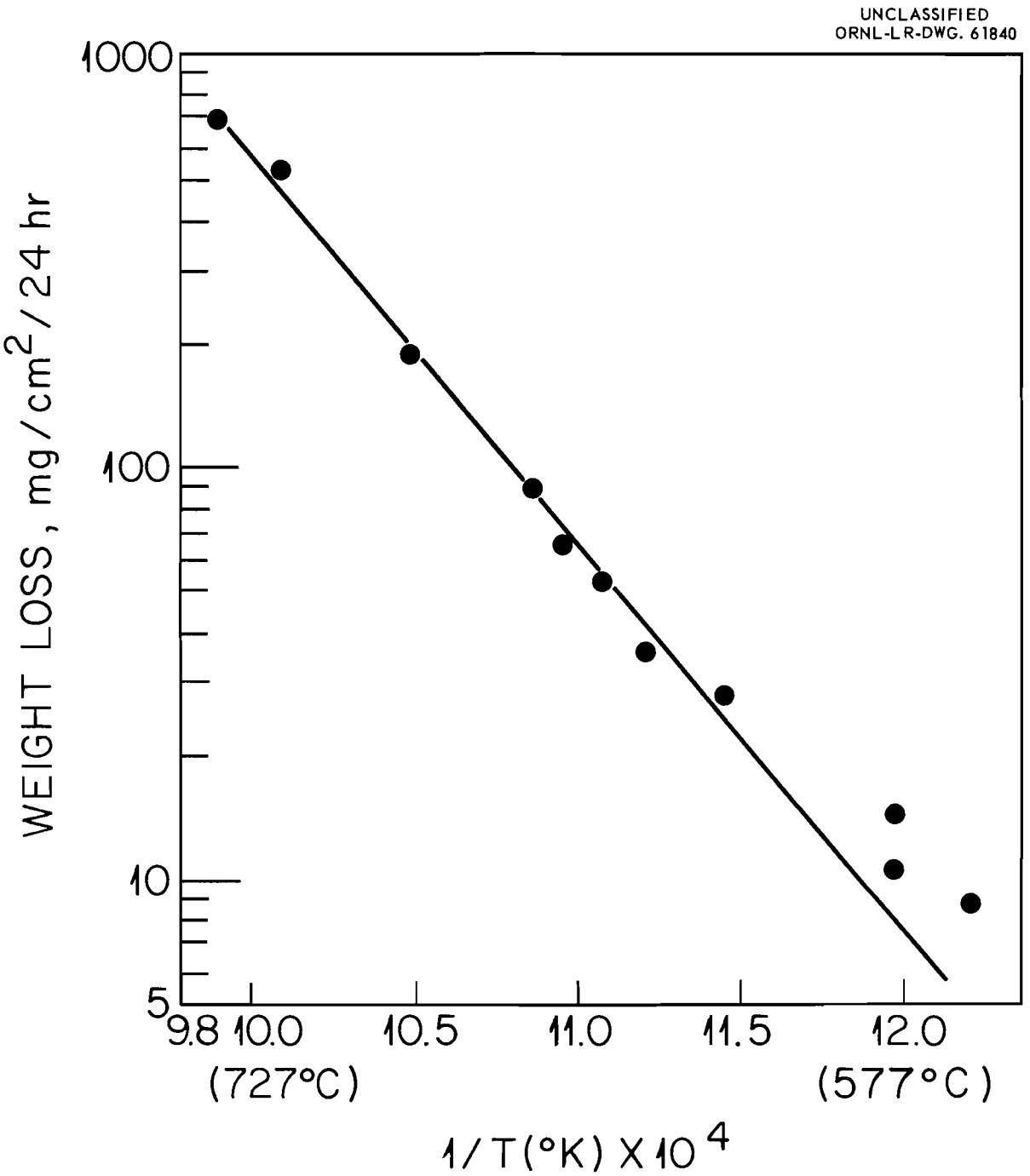

Fig. 11. Weight loss of Haynes Alloy 25 observed at various temperatures during passage of nitrogen-carbon tetrachloride mixture through the hydrochlorinator reaction vessel.

Table 14. Corrosion of Welded Specimens of Type 347 Stainless Steel in a Simulated Plutonium Solvent Extraction Solution[a] at 103°C

Test Period (hr)	Corrosion Rate (mpm)		
	V	I	S
96	<0.01	0.01	0.02
	0.02	<0.01	0.02

[a]Solution contained 1.0 M HNO_3, 2.0 M acetic acid, 45 g/liter of $UO_2(NO_3)_2 \cdot 6H_2O$

3.4 Graphite Fuel Decomposition Studies

One method proposed for processing graphite-uranium and uranium carbide fuels is to disintegrate-leach in boiling 90% (20 to 21 M) HNO_3.

Welded specimens of titanium-45 A were exposed in solution, interface, and vapor of a boiling solution consisting of 20 M HNO_3, 50 g U/l and 20 g of solid graphite per liter. No evidence of attack or staining was observed on any of the specimens after exposures of as long as 144 hr. Maximum rates for this exposure time were 0.03 mil/mo (Table 15). Titanium appears, therefore, to be an eminently satisfactory material of construction for a dissolver in this system, provided that fluoride is not added in subsequent processing steps. Because of the possibility of such addition in certain flowsheets, other materials will be evaluated in this system.

Table 15. Corrosion of Titanium-45A in Solutions[a] Encountered During Disintegration-Leach Process for Graphite-Uranium Fuels

Test Period (hr)	Corrosion Rate (mpm)		
	V	I	S
24	0.11, 0.09	0.11, 0.14	0.10, 0.17
48	0.04, 0.05	0.06, 0.09	0.06, 0.09
72	0.03, 0.04	0.04, 0.06	0.04, 0.06
144	0.03, 0.01	0.02, 0.04	0.03, 0.03

[a]Solution contained 20.0 M HNO_3, 50 g/liter U, and 20 g/liter graphite.

3.5 Darex System

Welded specimens of Haynes 21 and Haynes 25 exposed in boiling 5 M HNO_3-2 M HCl corroded at maximum rates of 3-10 and 0.31 mils/mo, respectively (Tables 16 and 17). All solution and interface specimens showed signs of intergranular attack. The unexpectedly poor resistance of Haynes 21 compared to the Battelle results (14) is believed to be due to the mill anneal which was given the specimens used in the current test. The test will be repeated on specimens which have been subjected to various types of quenching following heat treatment.

3.6 Transuranium Reprocessing System

The processes currently planned for the isolation of the transuranium elements make use of concentrated chloride solutions covering a wide range of acidities. In some steps nitrate will also be present. In all solutions containing appreciable concentrations of the transuranium elements, peroxide is expected to be present as a product of the radiolysis of water. It is expected that the most difficult environment to contain will be HCl in a container which contains radioactivity periodically.

Tests lasting from 24 to 840 hr have been run on ten materials in a number of solutions which have been proposed at some point in the flowsheet. The results are summarized in Table 18 in which the maximum corrosion rate observed is listed regardless of the specimen position (solution, interface, or vapor). It will be observed that crystal bar zirconium performed well in 6 M HCl at 105°C both in the presence and absence of 0.0015 M H_2O_2, 0.7 and 0.1 mil/mo, respectively, though the test in the presence of peroxide needs

Table 16. Corrosion of Welded[a] Specimens of Haynes 21 Alloy in Refluxing Initial Darex Solutions[a]

Test Period (hr)	Specimen Condition	Corrosion Rate (mpm)		
		V	I	S
48	Welded; heat-treated	0.94, 0.48	1.64, 1.26	1.59, 1.58
	As-welded	2.23, 0.66	3.74, 8.49	4.27, 3.08
96	Welded; heat-treated	0.80, 0.38	2.21, 1.50	2.10, 2.02
	As-welded	2.46, 1.21	3.76,16.63	6.51, 4.80
144	Welded; heat-treated	0.87, 0.38	0.79, 1.80	2.64, 2.54
	As-welded	3.47, 1.71	5.16,17.54	8.80, 6.50
192	Welded; heat-treated	0.88, 0.39	3.27, 2.09	3.12, 3.00
	As-welded	5.20, 2.13	5.77,17.56	10.03, 7.41

[a]Solution composed of 5.0 M HNO_3-2.0 M HCl.

Table 17. Corrosion of Welded Specimens of Haynes 25 Alloy in Refluxing Initial Darex Solution[a]

Test Period (hr)	Specimen Condition	Corrosion Rate (mpm) V	I	S
48	Welded; heat-treated	0.13, 0.13	0.23, 0.23	0.24, 0.25
	As-welded	0.16, 0.16	0.25, 0.25	0.28, 0.29
96	Welded; heat-treated	0.10, 0.11	0.22, 0.22	0.23, 0.24
	As-welded	0.14, 0.14	0.23, 0.23	0.27, 0.28
168	Welded; heat-treated	0.09, 0.10	0.23, 0.24	0.25, 0.26
	As-welded	0.14, 0.15	0.23, 0.23	0.29, 0.31
264	Welded; heat-treated	0.10, 0.10	0.25, 0.27	0.28, 0.29
	As-welded	0.13, 0.13	0.22, 0.21	0.29, 0.31

[a]Solution composed of 5.0 M HNO_3- 2.0 M HCl.

to be continued for much longer than the 48 hr reported. Hastelloy B showed a rate of 6.7 mils/mo in this same environment. The high cobalt alloys, Haynes 21 and Haynes 25, which are known to perform fairly well in dilute aqua regia do very poorly (38 and 29 mils/mo, respectively) in oxygenated HCl. In acid waste solutions (0.6 M HNO_3, 0.3 M HCl, 0.6 M $Al(NO_3)_3$, 3.6 M LiCl, 0.003 M $RuCl_3$ at 43°C) both Types 304L and 309 SCb showed rates of greater than 500 mils/mo vs 0.5 for Hastelloy C, 0.6 for Haynes 21, 0.1 for Haynes 25, 3.4 for zirconium, 0.1 for titanium 55A and 10.9 mils/mo for Hastelloy F. In neutralized waste all of these materials showed maximum rates of less than 0.1 mil/mo.

From these data zirconium and Zircaloy 2 appear to be the most generally satisfactory materials of construction for parts of the system which will handle HCl both with and without H_2O_2 but only in the absence of appreciable amounts of nitric acid (13.8 and 312 mils/mo). Hastelloy B is known to be reasonably resistant to HCl and will be subjected to further tests to determine whether or not its fairly good resistance to 6 M HCl-0.0015 M H_2O_2 continues for longer exposure times and higher peroxide concentrations.

4.0 MECHANISMS OF SEPARATIONS PROCESSES - FOAM SEPARATION (Subcontract 2024 with Radiation Applications, Inc) (W. Davis, Jr.)

4.1 Surface Chemistry of Dodecyl Benzene Sulfonate (E. Schonfeld)

The surface chemistry of dodecyl benzene sulfonate (DBS) is being studied in some detail because this surfactant shows considerable potential for

Table 18. Summary of Corrosion Tests for Transuranium Processing Facility

Material	Maximum Corrosion Rate, mils/mo							
	6 M HCl 0.0015 M H_2O_2 flowing 105°C (48 hr)	3 M HCl oxygenated 43°C (168 hr)	6 M HCl non-aerated 105°C (24-72 hr)	3 M HCl; 1 M HNO_3 oxygenated 43°C (168 hr)	6 M HCl-8 M HNO_3 non-aerated 105°C (24-72 hr)	8 M HNO_3 oxygenated 43°C (168 hr)	0.6 M HNO_3 0.3 M HCl 0.6 M $Al(NO_3)_3$ 3.6 M LiCl 0.003 M $RuCl_3$ oxygenated 43°C (168-840 hr)	8 M HNO_3 non-aerated 43°C (168 hr)
304L stainless							1050*	
309 SCb stainless							502*	
Hastelloy B	6.7							
Hastelloy C		10.5		0.9		3.6**	0.5**	2.4
Hastelloy F							10.9	
Haynes 21		38				0.1	0.6	
Haynes 25		29			3.2	0.1	<0.1	
Zr (cryst bar)	0.7	0.1	0.1		312	<0.1	3.4	
Zr-2	0.9		0.1		13.8			
Ti-55A	Dissolved		Dissolved		3.1		<0.1	
Multimet			496		523			
Illium W			36		163			

*25 hr exposure time

**840 hr exposure time.

separating strontium from certain waste solutions. A series of experiments was performed to compare dynamic and static values of the saturated surface concentration of DBS. In the static tests, surface tensions of DBS in water and in 0.1 M NaCl solution were measured to determine the value of n (=1 or 2) the number of thermodynamically significant species, in the Gibbs equation

$$d\gamma = -\Gamma_1 RT \, d \ln a_1 - \Gamma_2 RT \, d \ln a_2, \qquad (1)$$

where γ is the surface tension of the solution, Γ_1 and Γ_2 are the excess surface concentrations of the sulfonate and its cation (Na^+), respectively, a_1 and a_2 are corresponding activities, R and T have their usual meanings. The quantity n equals unity for the salt solution since a change of concentration of DBS in the range 10^{-5} to 10^{-3} M, i.e., the range that is significant in foaming, has essentially no effect on the activity of the Na^+ ion in the 0.1 M NaCl solution. Hence, in this case, $d \ln a_2/d \ln a_1 = 0$, and equation 1 reduces to

$$\frac{-d\gamma}{d \ln a_1} = \Gamma_1 RT. \qquad (2)$$

When the sulfonate ion and sodium ion concentrations are equal, as in the case of DBS in water, then $d \ln a_2/d \ln a_1 = 1$, in which case

$$\frac{-d\gamma}{d \ln a_1} = 2 \Gamma_1 RT, \qquad (3)$$

if the Na^+ concentration is thermodynamically significant.

Surface tension versus log (DBS) plots give the same value, namely 3.4×10^{-10} moles/cm^2 for the monolayer concentration for both water and 0.1 M NaCl solutions of DBS. Thus, the term Γ_2 RT dln a_2 in equation 1 must be eliminated, i.e., n = 1. Physically, this means that the sesquestering tendency of the sodium form of DBS is due to a molecular species, not to an anionic sulfonate plus a metal ion.

Dynamically, the saturated surface concentration of DBS was determined by using a single stage foam separation column. From 60 measurements of the equilibrium surface concentration,* averages of which are plotted in Fig. 12, corresponding to bulk phase concentrations of 0.2 to 4.5×10^{-3} moles DBS/l, the surface excess at saturation is 3.1×10^{-10} moles/cm^2. This value agrees well with that determined in the static experiments. In addition to concentration of DBS, three different gas flow rates were used to assure that no refluxing was occurring. Bubble diameters were all in the range 0.40 to 0.48 mm.

*The DBS concentration in bulk and foam condensate phases was measured by ultra violet spectrophotometry. At 2235 and 2610 A this surfactact follows Beer's law with respective molar extinction coefficients, ϵ, of 10^4 and 410. These values are also independent of pH in the range 3 to 11.

The constancy of the surface excess at bulk phase concentrations higher than the critical micelle concentration (CMC) of ~2.2 x 10^{-3} moles/l, Fig. 12, shows that the Gibbs equation cannot be used beyond this point. This surfactant is very useful in studies of the mechanism of foaming since it forms stable foams at concentration $\leq$4% of the CMC (Fig. 12). Many surfactants do not foam well as concentrations less than 50% of the CMC.

4.2 Low Level Waste Decontamination

Three approaches are being studied in efforts to apply the foam separation process to the decontamination of ORNL Low Level Waste: (1) removal of calcium, strontium, and cesium by foaming; (2) complexing of calcium by EDTA, or other agents, thereby holding calcium in solution while strontium and cesium are removed by foaming; (3) partial precipitation of calcium and strontium by addition of sodium carbonate, sodium hydroxide, or sodium phosphate, removing the solids by flotation and then the soluble cations by foaming. Cesium would be removed by adding finely divided clay, which strongly sorbs cesium, or ferrocyanide, which forms a solid with cesium, during the flotation phase.

Experiments were performed on portions of each of these methods. Those on method 3 consisted of adding tracer strontium and sodium hydroxide to ORNL tap water, which has nearly the same macroscopic composition as the low level waste, removing the resulting calcium-strontium precipitate by filtration, which was used instead of the flotation step, and then removing soluble strontium tracer by foaming with dodecyl benzene sulfonate as the surfactant. In two tests with tap water made 5 and 10 x 10^{-3} molar in sodium hydroxide, approximately 90% of the strontium and calcium (Table 19) precipitated. To each of the resulting filtrates 62 mg DBS/liter was added and the strontium distribution coefficient determined in a single stage foam column. The strontium distribution coefficients, ~2.5 x 10^{-3} cm, were large enough to suggest that ORNL low level waste could be decontaminated with respect to strontium in a countercurrent foam column after removal of most of the calcium. For example, a distribution coefficient of 2.5 x 10^{-3} cm in a foam column of ~20 theoretical stages corresponds to a decontamination factor >100, a volume reduction factor of ~100, and a liquid throughput of ~50 gal ft^{-2} hr^{-1} when the bubble diameter is 0.5 mm.

Experiments were also performed to help define an optimum concentration of the surfactant DBS on strontium removal by foaming and the effect of calcium concentration on the distribution coefficient (Table 20). Calcium concentrations were 0.4 to 4 ppm, corresponding to the partial removal of this element either by precipitation, flotation, or complexing with EDTA; surfactant concentrations ranged from 62 to 250 mg/liter (or ppm). The maximum separation of strontium Γ/x = 2.0 x 10^{-2} cm, occurred with a solution containing 10^{-3} M NaOH, no calcium, and a DBS concentration of 62 mg/liter. However, the strontium distribution coefficient is still acceptably high, 1.25 x 10^{-3} cm, in the presence of 4 ppm Ca^{++}. Increasing the DBS concentration to 125 mg/liter, at a pH of 12, produced only a small increase in Γ/x.

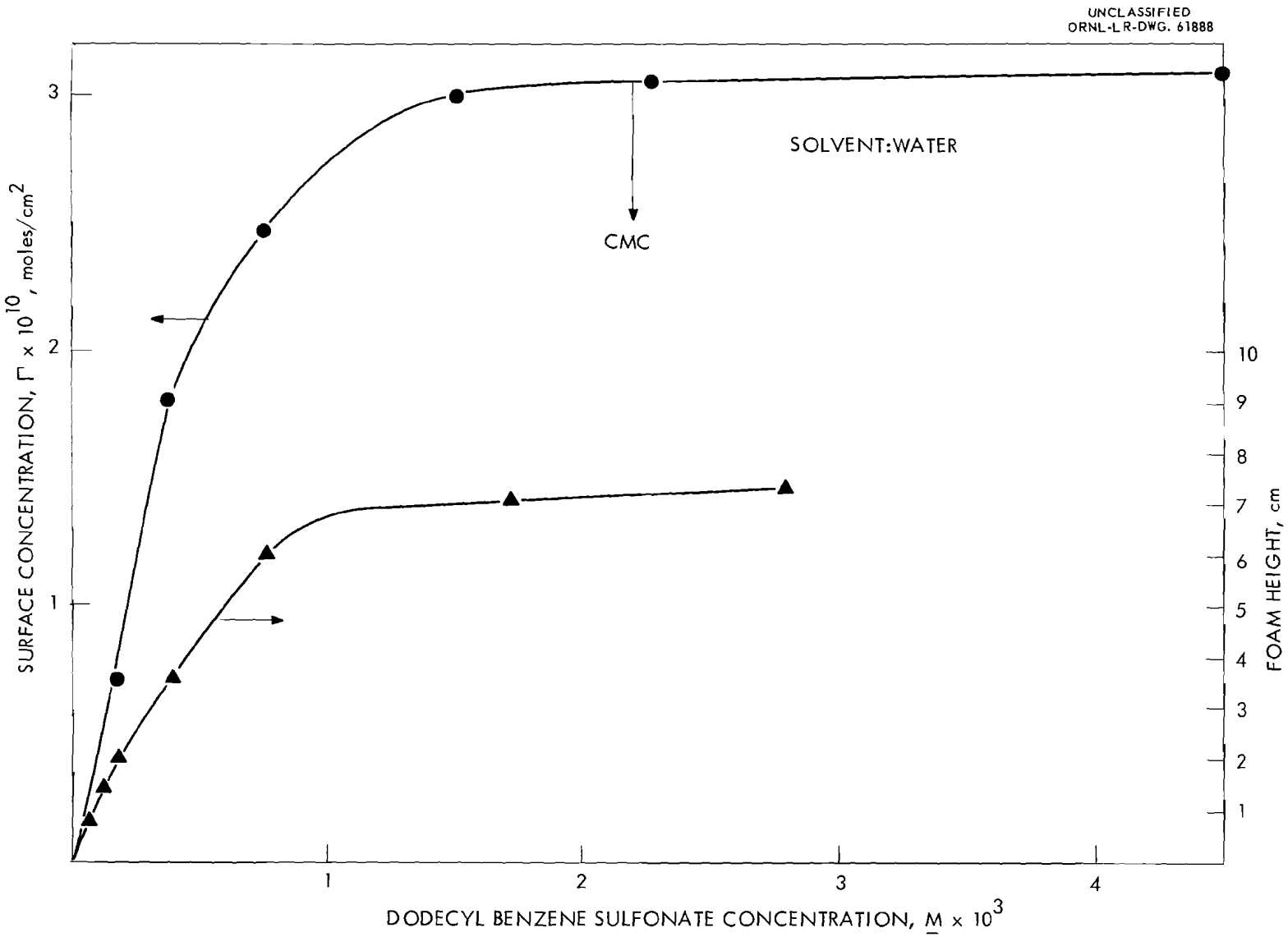

Fig. 12. Effect of bulk phase concentration on the surface concentration and foam stability of dodecylbenzene sulfonate solutions.

Table 19. Precipitation of Calcium from ORNL Tap Water with Sodium Hydroxide

NaOH Conc Added to Tap Water x 10^3, moles/liter	Solution pH	Residual Ca^{++} After 24 hr Settling, ppm
0	7.7	27
1	9.3	9.5
2	10.3	5.0
5	11.2	3.0
10	11.7	2.0

Table 20. Strontium Distribution Coefficients in Alkaline ORNL Tap Water with the Surfactant Dodecyl Benzene Sulfonate (DBS)

Surfactant Conc, mg/l	Sr^{++} Conc x 10^6, moles/l	NaOH Conc x 10^3, moles/liter	pH	Ca^{++} Conc, ppm	Sr^{++} Distribution Coefficient, $(\Gamma/x) \times 10^3$ cm
250	2	1	~11	0	17.
62	1	1	~11	0	20.
62	1	10	~12	0	8.7
62	1	10	~12	0.4	8.5
62	1	10	12	2.0	2.2
62	1	10	12	4.0	1.25
125	1	10	12	4.0	1.40

5.0 WASTE TREATMENT
(W. E. Clark)

5.1 Phosphate Glasses (H. W. Godbee)

Simulated TBP-25 was incorporated into melts at 875-1000°C. On cooling, either quenched or annealed, the melts gave glassy solids with densities of 2.36 to 2.84 g/ml representing volume reduction factors from 7.6 to 8.4. One of the more satisfactory mixtures from consideration of behavior during heating, softening point, fluidity of melt, and quality of final product, gave a glass with 40.5, 25.0, 18.6, and 15.9 wt %, respectively, of P_2O_5, Al_2O_3, Na_2O, and PbO (15).

Fluxing agents used to form melts were borate and lead oxide. Borate was added as tetraborate, $B_4O_7^{2-}$, and lead oxide as PbO. Lead oxide did not lower the viscosity and softening point of melts as well as borate. However, a big advantage of lead oxide is that it does not cause foaming of the solid prior

to melting as does borate. Another advantage of lead oxide is that it gives a better density of melt to weight of added oxides ratio than other additives studied. The higher this ratio the greater is the volume reduction obtained. Other additives briefly investigated were magnesia and silica. Silica has the distinct disadvantage that it forms a precipitate in the original solution. Phosphate was added as sodium hypophosphite, NaH_2PO_2, to the extent of two moles per liter of TBP-25 waste.

5.2 Ruthenium Volatility (H. W. Godbee)

Experiments were performed to study the effect of hypophosphite on ruthenium volatility and noncondensable off-gas production during evaporation-fixation. The experiments were carried to about 1000°C in small all-quartz equipment described previously (16) with a 200 ml stainless steel beaker for a pot. Simulated high-activity TBP-25 waste containing 0.027 mg/ml stable ruthenium and 0.1 μc/ml Ru-106 tracer were used.

In two experiments, 2.0 moles sodium hypophosphite, $NaH_2PO_2 \cdot H_2O$ were added per liter of waste. Ruthenium in the condensate was 0.48 and 0.71%, respectively, of the original ruthenium. In a third experiment 2.0 moles $NaH_2PO_2 \cdot 2H_2O$ plus 0.25 mole $Pb(NO_3)_2$ were added per liter of waste. Ruthenium in the condensate was 2.18% of the original. In a fourth experiment 2.0 moles $NaH_2PO_2 \cdot H_2O$ plus 0.25 mole PbO were added per liter of waste. Ruthenium in the condensate was 0.68% of the original. The latter two experiments were to determine if addition of a lead fluxing agent has a deleterious effect on ruthenium volatility. In none of the experiments was any detectable net off-gas produced.

These results show that ruthenium in the condensate can be held to less than one per cent by addition of at least two moles of sodium hypophosphite per liter TBP-25. Also they indicate that increased nitrate, from $Pb(NO_3)_2$, increases ruthenium in the condensate while decreased acid, by PbO addition, does not materially effect ruthenium in the condensate.

5.3 Nitrate-Phosphite Reaction (W. E. Clark, H. W. Godbee and K. L. Servis)

Experiments to determine the nature of the products from the reaction between the nitrate and phosphite ions were carried out in all-glass equipment previously described (17). In the experiments using salt nitrates and orthophosphorous acid the evolution of noncondensable gases started at a higher temperature, 120-130°C compared to ~110°C, than in the previous experiments with nitric and phosphorous acids 15 and 17. When the gas evolution from salt nitrate-phosphorous acid mixtures started, the distillate was more than 6 N HNO_3. The nature of the noncondensable gases was not significantly different from that of the previous HNO_3-H_3PO_3 reactions (17). The principal gaseous reaction product was nitric oxide (NO).

A series of exploratory experiments were performed to investigate the catalysis of the reaction between nitrate and phosphite. In each experiment, 0.0005-0.01 mole of the material under investigation was added to the reaction mixture. The best catalysts for the reaction between nitrate ion and phosphate ion were found to be the silver, mercuric, and palladium ions. All of these cations are reduced by orthophosphorous acid to the free metal, while the free metals are all oxidized by nitric acid. The cations (15) which did not catalyze the reaction are either not reduced by phosphorous acid or are not oxidized by nitric acid.

5.4 Waste Solution Vapor-Liquid Equilibrium Data (W. E. Clark, H. W. Godbee)

Vapor-liquid equilibrium conditions were investigated for representative TBP-25, Darex and high sulfate Purex simulated waste solutions by means of Gillespie still distillations. Vapor-liquid equilibrium data were obtained as a function of acid concentration and salt concentration. The effect of pressure (atmospheric and 180 mm Hg vacuum) on the systems was also measured. Densities of the pot solutions were measured at 25, 50, 75, and 100°C (15).

5.5 Low Level Waste Treatment (R. R. Holcomb)

An eighth demonstration run in the semi-pilot plant facility has been completed. The preliminary results indicate excellent decontamination factors >1000 for Sr, 100 for TRE and >100 for Cs prior to Cs breakthrough at ~1500 bed volumes. Overall volume reduction was slightly less than 3000. Neither Sr nor total hardness breakthrough were detected up to 2000 bed volumes. Total hardness in the overflow from the clarifier averaged about 20 ppm as compared to 60 ppm in the previous run in which a premature breakthrough of activity and hardness occurred at ~600 bed volumes. These results support the hypothesis that the early breakthrough in Run 7 was caused by a carbonate deficiency in the water resulting in precipitation of the more soluble $Ca(OH)_2$ rather than $CaCO_3$. The soluble calcium saturated the resin and allowed a breakthrough of activity. Continuous analysis of the effluent for total hardness will detect any future breakthroughs of this type and allow time to remedy the cause by addition of carbonate to the water before significant fractions of activity are discharged.

The results of these runs has been reported in more detail (18) and are presently being incorporated into a comprehensive topical report.

6.0 ION EXCHANGE
(W. Davis, Jr.)

6.1 Fission Product Recovery by Ion Exchange (W. C. Yee)

It was previously (19) shown that >85% of the ~1 M $SO_4^{=}$ in Purex 1WW can be precipitated by the addition of excess ferric ion, as $Fe_2O_3 \cdot xH_2O$ or partially dehydrated $Fe(NO_3)_3 \cdot 9H_2O$, after the 1WW has been made 50-55% in

HNO_3 by the addition of fuming nitric acid. After concentrating the nearly-sulfate-free filtrate by evaporation and increasing the HNO_3 concentration ~63%, a precipitate was obtained that contained ~85% of the original strontium, <10% of the original iron, ~30% of the original aluminum, and some of the rare earth fission products. This strontium-rare earth concentrate is being used as a source material for further development of the ion exchange process for strontium recovery previously described (20).

In the first test, one batch of precipitate was dissolved in 8 M HNO_3, made 0.03 M in oxalic acid to complex iron, and then diluted by a factor of 10. The resulting solution was passed through a column of Dowex 50W-X8 (20-50 mesh) resin at the high flow rates associated with water demineralization, i.e., a linear velocity of 3 cm/min, or 15 ml/min in the experimental column. This high flow rate was chosen to minimize holdup time, which would be significant in process use from the standpoint of radiation degradation. The column was then eluted at these same high flow rates, first with 29 resin volumes of 0.25 M monosodium citrate, pH 3.6, then with 32 resin volumes of 0.13 M sodium versenate, pH 6.0.

Radiochemical analyses of the solutions from the resin column showed that at the high flow rates of this experiment equilibrium was not attained in either the sorption or elution cycles. On the sorption cycle, ~97% of the rare earths were sorbed but only ~40% of the strontium. Elution with 29 resin volumes of 0.25 M monosodium citrate removed only ~75% of the rare earths and also removed 15% of the sorbed strontium; the sodium versenate eluted the remaining strontium and rare earths (Fig. 13). Both phases of the elution cycle showed the "tailing off " typical of incomplete and slow reaction. This experiment has shown that slower sorption and elution rates as well as finer mesh resin should be tested.

6.2 Radiation Damage to Ion Exchange Resin (W. C. Yee)

Analyses of Amberlite 200 (Table 21) previously irradiated (19) to 0.97×10^9 r (2.6 watt-hr/g dry resin) indicated that its original capacity (by titration) had decreased by 34%, moisture content had increased from 53% to 57%, median pore diameter had increased from 250 Å and 315 Å and surface area had increased from 50 to 60 m^2/g dry resin. From the original and final values of sulfur content and densities, the radiolytic loss of sulfur, G(-S), was calculated to be 1.2 atoms/100 ev of γ-radiation absorbed by the resin.

The loss in capacity of Amberlite 200, a highly crosslinked (not specified by the manufacturer) yet porous resin, was comparable to that of Dowex 50W X-8 resin, which lost 30% of its original capacity after an exposure of 0.85×10^9 r (2.3 watt-hr/g dry resin). The weight loss of 14% (Table 21) also compares well with the 12% weight loss of the Dowex resin. No comment can be made at this time on the significance of the increase in moisture content because its relationship to change in crosslinkage in a highly porous resin is probably different from that of a conventional resin such as Dowex 50W.

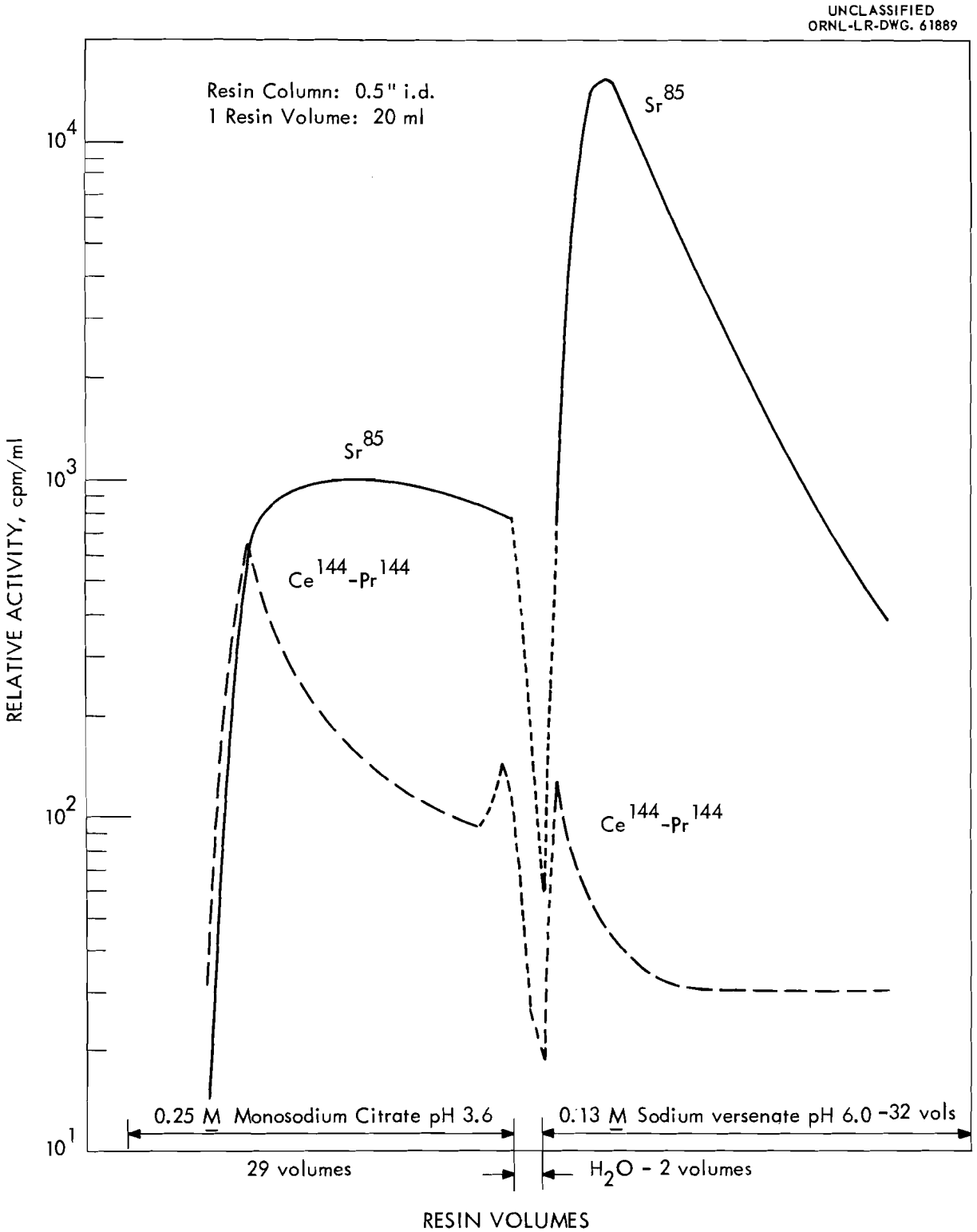

Fig. 13. Elution of Ce^{144}-Pr^{144} and Sr^{85} at high flow rates - 15 ml/min, 3 cm/min.

Table 21. Summary of Data on Irradiated* Amberlite 200 (16-50 mesh)

	Original Resin	One Week Irradiated
Resin density, g dry resin/ml wet resin	0.368	0.321
Resin volume lost, vol %	-	2%
Resin weight lost (dry basis), %	-	14%
Surface Area, m^2/g dry resin	49.9	59.7
Median Pore Diameter, Å	250	315
Void Fraction	0.322	0.297
Moisture Content, wt %	53.0	57.2
Sulfur Content, wt %	14.8	12.6
Capacity, meq/g dry resin		
by titration	5.00	3.30
by sulfur analysis	4.62	3.93

*Irradiated to 2.6 watt-hr/g dry resin (0.97×10^9 r) in a field of 0.013 watts/g dry resin.

7.0 CHEMICAL APPLICATION OF NUCLEAR EXPLOSIONS
(W. D. Bond)

Work has continued on studies of tritium exchange in the reaction, $HTO + H_2 \longrightarrow H_2O + HT$, with several compounds that are present in rock salt. Calcium sulfate was studied in some detail and scouting experiments were made on NaCl, K_2SO_4, Al_2O_3, K_2SO_3, $CaCl_2$ and silica gel. Studies were made by passing a mixture of H_2-HTO-H_2O through fixed beds of catalysts and measuring the amount of HT formed. Further work was performed on the reduction of magnesium and of calcium sulfate by hydrogen to elucidate the mechanism of the reduction.

7.1 Tritium Exchange

A number of compounds which may be present in rock salt were tested for their effectiveness as catalysts for vapor phase exchange in the H_2-H_2O-HTO system (Table 22). The comparative tests were made by flowing the gaseous mixture through 1 in. dia beds that were 6 in. long using flow rates of 6.5×10^{-3}, 4.5×10^{-4} and 4.1×10^{-11} moles/min of H_2, H_2O, and HTO, respectively. The chlorides were not very effective catalysts under conditions of the experiment, while oxygenated salts and oxides tried in the form of large crystals were at least moderately effective. This is consistent with the view that

Table 22. Steady State Exchange for the Reaction, $HTO + H_2 = HT + H_2O$ Over Fixed Beds of Solid Catalyst

Initial Flow Rates, moles/min: $H_2 = 6.5 \times 10^{-3}$
$H_2O = 4.5 \times 10^{-4}$
$HTO = 4.1 \times 10^{-11}$

Substance	Surface, Area, m^2/g	% of Equilibrium Exchange
NaCl	0.015	0.65
$CaCl_2$	0.39	6-7
K_2SO_4	0.009	42.5
Silica gel	520	44
Al_2O_3	6.7	77
K_2CO_3	0.073	80
"Drierite"[a]	9.7	95

[a]Made from naturally occurring anhydrite, $CaSO_4$.

exchange involves adsorption of one or all of the reactants on a surface which contains exposed oxygen atoms. In the case of chlorides the exchange is believed to involve reversible hydrolysis of the chlorides. It is not completely certain that the measured exchanges involve only the chemical nature of the solids, rather, in some cases, it may reflect surface area differences among the compounds.

In an attempt to demonstrate the kinetics and mechanism of the exchange several experiments were performed with $CaSO_4$ powders (325 mesh). The exchange was not a simple function of surface area of the powders. With $CaSO_4$ powders having surface areas of 1.3, 10.0, and 0.82 m^2/g in fixed bed depths of 3/32 in. the T exchange at 600°C was 0, 9.0, and 5.2%, respectively. The anomalous surface area behavior is believed to be a result of the powders acting as a single plug with more "canneling" when packed in the furnace tube. This conclusion was reached after experiments with upflow of the reactant gases showed that the bed did not fluidize but floated as a single plug. Larger particle sizes will be prepared for future experiments.

7.2 Reduction of Sulfates by Hydrogen

Further work was performed on $CaSO_4$ and $MgSO_4$ to demonstrate the mechanism of the reductions. Experimental evidence to date indicate the mechanism of the reductions involves the following reductions:

$$MeSO_4 + H_2 \longrightarrow MeSO_3 + H_2O \quad (1)$$

$$MeSO_3 \longrightarrow MeO + SO_2 \quad (2)$$

$$7H_2 + 3SO_2 \longrightarrow 6H_2O + H_2S + S_2 \quad (3)$$

$$3/2\ S_2 + 2MeO \longrightarrow 2\ MeS + SO_2 \quad (4)$$

$$4MeO + 6\ SO_2 \longrightarrow 4Me\ SO_4 + S_2 \quad (5)$$

$$MeS + H_2O \longrightarrow H_2S + MeO \quad (6)$$

where: Me = metal ion

The final reduction products of $CaSO_4$ were CaS, CaO, H_2O and H_2S where as the final reduction products of $MgSO_4$ were MgO, S, H_2S, SO_2, and H_2O. SO_2 and S_2 could not be detected in the off-gas of $CaSO_4$ reductions nor could MgS be detected in the solid product from $MgSO_4$ reductions.

The proposed equations for the mechanism of reduction of the sulfates are supported by the following experimental observations:

1) $MgSO_3$ is thermally decomposed very rapidly below reduction temperature. $CaSO_3$ slowly decomposes at reduction temperatures.

2) H_2 and SO_2 react rapidly (eq. 3) at reduction temperature when catalyzed by MgO or CaO. MgO remains unchanged after the reaction but CaO is largely converted to CaS and $CaSO_4$. This could explain the reason why no SO_2 or S_2 is observed in $CaSO_4$ reduction and why MgS is not formed in $MgSO_4$ reductions.

3) Hydrolysis of the sulfates by steam is much too low to be important in the mechanism.

4) CaO is mostly formed by eq. 2 rather than by hydrolysis with the product H_2O since less than 1% of the sulfide is decomposed after passing H_2O at a flow rate of 25 mg/min over 1 g of CaS for 2 hr at the reduction temperature of the sulfate.

5) Reaction of MgO and SO_2 (eq. 5) is practically nil whereas that of CaO and SO_2 is rapid to form $CaSO_4$ and CaS.

It is concluded from the experimental evidence that sulfates are first reduced to sulfites which subsequently decomposed to the oxide and SO_2. The final products then depend on the thermodynamics of the interactions among the metal oxide, H_2O, H_2, and SO_2.

8.0 REFERENCES

1. M. J. Bradley and L. M. Ferris, Ind. Eng. Chem., 53, 279 (1961).

2. "Fuel Element Development Program for the Pebble Bed Reactor," NYO-9064 (April 30, 1961).

3. L. M. Ferris, A. H. Kibbey, and M. J. Bradley, "Processes for Recovery of Uranium and Thorium from Graphite Fuel Elements. Part II." ORNL-3186 (in press).

4. "Proceedings of the Uranium Carbide Meeting Held at ORNL, Dec. 1-2, 1960," TID-7603.

5. "Quarterly Progress Report for Chemical Development Section B, April-June 1961," ORNL-CF-61-8-50 (in press).

6. W. E. Clark, J. R. Flanary, and F. G. Kitts, "The Darex Process: The Treatment of Stainless Steel Reactor Fuels with Dilute Aqua Regia," ORNL-2712 (in preparation).

7. W. E. Clark and T. A. Gens, "A Study of Dissolution of Reactor Fuels Containing Zirconium in a Titanium Vessel," ORNL-3118 (in press).

8. F. G. Kitts, "The Use of Boron for Fluoride Complexing in Thorex Dissolver Solutions," ORNL-59-8-29 (August 1959).

9. T. A. Gens, "Dissolution of Zirconium Fuels in Darex Titanium Equipment," TM-22 (in press).

10. O. W. Parrett, "Modifications for the STR Fuel Recovery Process," IDO-14522 (Dec. 1, 1960).

11. Personal communication with M. E. Weech of ICPP.

12. R. H. Rainey, A. B. Meservey, and R. A. Mansfield, "Laboratory Development of the Thorex Process Progress Report, Dec. 1, 1955 to Jan. 1, 1958," ORNL-2591 (Feb. 11, 1959).

13. "Quarterly Progress Report for Chemical Development Section B, April-June 1961," ORNL-CF-61-8-50 (in press).

14. P. D. Miller, C. L. Peterson, E. L. White, F. W. Fink, "Evaluation of Container Materials for Zircex and Darex Nuclear Fuel Recovery Processes," BMI-1242, pp. 30-36 (Dec. 11, 1957).

15. "Waste Treatment and Disposal Progress Report for August and September 1961," (in preparation).

16. "Waste Treatment and Disposal Progress Report for April and May 1961," ORNL-CF-61-7-3 (Aug. 1, 1961).

17. "Waste Treatment and Disposal Progress Report for June and July 1961," ORNL-TM-15 (Oct. 24, 1961).

18. "Waste Treatment and Disposal Progress Report for August and September 1961," (in preparation).

19. "Quarterly Progress Report for Chemical Development Section B, April-June 1961," ORNL-CF-61-8-50 (in press).

20. "Chemical Technology Division Annual Progress Report for Period Ending August 31, 1960," ORNL-2993 (Sept. 26, 1960).

DISTRIBUTION

1. J. B. Adams
2-3. R. E. Blanco
4. J. O. Blomeke
5. J. C. Bresee
6. K. B. Brown
7. W. E. Clark
8. F. L. Culler
9. W. Davis
10. L. M. Ferris
11. D. E. Ferguson
12. J. R. Flanary
13. T. A. Gens
14. H. E. Goeller
15. A. D. Goldman
16. J. M. Googin
17. A. T. Gresky
18. C. E. Guthrie
19. P. A. Haas
20. F. E. Harrington
21. R. F. Hibbs
22. J. M. Holmes
23. R. W. Horton
24. A. R. Irvine
25. W. H. Jordan
26. F. G. Kitts
27. E. Lamb
28. W. H. Lewis
29. R. B. Lindauer
30. A. P. Litman
31. J. T. Long
32. J. P. Nichols
33. E. L. Nicholson
34. R. H. Rainey
35. J. T. Roberts
36. A. D. Ryon
37-39. E. M. Shank
40. M. J. Skinner
41. S. H. Smiley
42. E. G. Struxness
43. J. C. Suddath
44. J. A. Swartout
45. J. W. Ullmann
46. C. D. Watson
47. M. E. Whatley
48. C. E. Winters
49. R. G. Wymer
50. E. L. Anderson, AEC, Wash.
51. R. F. Benenati, General Atomics
52. S. Bernstein, Paducah
53. J. A. Buckham, ICPP
54. J. T. Christy, AEC, Hanford
55. F. R. Dowling, AEC, Wash.
56. R. A. Ewing, BMI
57. M. K. Harmon, Hanford
58. L. P. Hatch, Brookhaven
59. B. R. Harward, Atomics International
60. O. F. Hill, Hanford
61. K. K. Kennedy, ICPP
62. E. M. Kinderman, SRI
63. S. Lawroski, ANL
64. J. A. Lieberman, AEC, Wash.
65. J. A. McBride, ICPP
66. R. A. McGuire, ICPP
67. B. Manowitz, BNL
68. J. W. Morris, du Pont, Savannah River
69. H. Pearlman, Atomics International
70. W. H. Reas, Hanford
71. H. Schoen, RAI
72. C. M. Slansky, ICPP
73. J. I. Stevens, ICPP
74. C. E. Stevenson, ANL
75. K. G. Steyer, General Atomics
76. V. R. Thayer, du Pont, Wilmington
77. R. E. Tomlinson, Hanford
78. J. Vanderryn, AEC ORO
79. F. M. Warzel, ICPP
80. W. E. Winsche, du Pont, Savannah River
81. Document Reference Section
82-83. Central Research Library
84-88. Laboratory Records
89. ORNL-RC
90-104. DTIE